

1 **Altitude and life-history shape the evolution of**

2 ***Heliconius* wings**

3 Gabriela Montejo-Kovacevich¹, Jennifer E. Smith², Joana I. Meier¹, Caroline N.
4 Bacquet³, Eva Whiltshire-Romero¹, Nicola J. Nadeau² & Chris D. Jiggins¹.

5 ¹*Department of Zoology, University of Cambridge, Cambridge, UK, CB2 3EJ*

6 ²*Animal and Plant Sciences, University of Sheffield, Sheffield, UK, S10 2TN*

7 ³*Universidad Regional Amazonica de Ikiam, Tena, Ecuador*

8
9
10
11 **Running title:** "Evolution of *Heliconius* wings"

12 13 **Author contributions**

14 G.M.K., J.E.S., N.J.N and C.D.J. conceived the study. G.M.K., J.E.S. and C.N.B.
15 conducted fieldwork. G.M.K., J.E.S., J.I.M., and E.W.R collated the dataset and
16 conducted the analyses. All authors contributed to the writing of the manuscript.

17 18 **Acknowledgements**

19 We would like to thank all the *Heliconius* researchers and field assistants that have
20 contributed to the wing collection used in this study. We also thank Simon H. Martin
21 and Stephen H. Montgomery for useful comments on early versions of this
22 manuscript. G.M.K. was supported by a Natural Environment Research Council
23 Doctoral Training Partnership. J.E.S. was supported by the Scurfield Memorial
24 Bursary (University of Sheffield). Funding was provided to C.B. by the Spanish
25 Agency for International Development Cooperation (AECID, grant number
26 2018SPE0000400194). N.J.N. and C.D.J were supported by a Natural Environment
27 Research Council (grant number: NE/R010331/1, NE/R153436/1).

28 29 **Data accessibility**

30 All images are now available in the public repository Zenodo
31 (<https://zenodo.org/communities/butterfly/>)

32 All R and image analysis scripts are available on Zenodo
33 (DOI:10.5281/zenodo.3491029)

36 *Abstract*

37 Phenotypic divergence between closely related species has long interested biologists. Taxa
38 that inhabit a range of environments and have diverse natural histories can help understand
39 how selection drives phenotypic divergence. In butterflies, wing colour patterns have been
40 extensively studied but diversity in wing shape and size is less well understood. Here we
41 assess the relative importance of phylogenetic relatedness, natural history and habitat on
42 shaping wing morphology in a large dataset of over 3500 individuals, representing 13
43 *Heliconius* species from across the Neotropics. We find that both larval and adult
44 behavioural ecology correlate with patterns of wing sexual dimorphism and adult size.
45 Species with solitary larvae have larger adult males, in contrast to gregarious *Heliconius*
46 species, and indeed most Lepidoptera, where females are larger. Species in the pupal-
47 mating clade are smaller than those in the adult-mating clade. Interestingly, we find that
48 high-altitude species tend to have rounder wings and, in one of the two major *Heliconius*
49 clades, are also bigger than their lowland relatives. Furthermore, within two widespread
50 species we find that high-altitude populations also have rounder wings. Thus, we reveal
51 novel adaptive wing morphological divergence among *Heliconius* species beyond that
52 imposed by natural selection on aposematic wing colouration.

53

54 **Keywords:** *Heliconius*, phenotypic divergence, wing morphology, Lepidoptera,
55 sexual dimorphism, altitude

56

57 *Introduction*

58 Identifying the selective forces driving phenotypic divergence among closely related species
59 lies at the core of evolutionary biology research. Adaptive radiations, in which descendants
60 from a common ancestor rapidly fill a variety of niches, are ideal systems to investigate
61 morphological divergence (Schluter 2000). The study of adaptive radiations has revealed
62 that evolution often comes up with similar solutions for similar problems at the phenotypic
63 and genetic levels (Losos 2010; Marques et al. 2019). Speciose groups that have repeatedly
64 and independently evolved convergent adaptations to life-history strategies and
65 environments are good systems in which study selection drivers (Schluter 2000).
66 Nevertheless, adaptive phenotypic evolution is often complex and multifaceted, with more
67 than a single selective force in action (Maia et al. 2016; Nosil et al. 2018). For example in
68 birds, sex differences in plumage colouration are driven by intra-specific sexual selection,
69 while natural selection drives sexes towards more similar colourations (Dunn et al. 2015).
70 Integrative approaches that make use of tractable traits across well-resolved phylogenies
71 are needed to explore the selective forces driving phenotypic evolution.

72

73 Butterfly wing colouration has been the focus of considerable research effort and major
74 strides have been made towards understanding how and when evolution leads to complex
75 wing colour patterns, conferring aposematism, camouflage, or a mating advantage (Merrill et
76 al. 2012; Chazot et al. 2016; Nadeau et al. 2016). The dazzling diversity of butterfly colour
77 patterns among species has perhaps obscured the less conspicuous phenotypic diversity of
78 wing shapes and sizes, which are more often regarded as the result of sexual selection,
79 flight trade-offs or developmental constraints (Singer 1982; Allen et al. 2011), rather than
80 drivers of local adaptation and species diversification (Srygley 2004a; Céspedes et al. 2015;
81 Chazot et al. 2016). A recent review assessing the ecology of butterfly flight, identified
82 habitat, predators and sex-specific behaviours as the selection forces most likely driving
83 wing morphology variation, but highlighted the need for further phylogenetic comparative

84 studies that identify the adaptive mechanisms shaping wings (Le Roy et al. 2019).

85

86 Differences in behaviour between sexes have been identified as one of the main drivers of
87 wing aspect ratio and size sexual dimorphism in insects (Rossato et al. 2018a; Le Roy et al.
88 2019). In butterflies, males tend to spend more time looking for mates and patrolling
89 territories, while females focus their energy on searching for suitable host plants for
90 oviposition (Rossato et al. 2018b). The same wing trait can be associated with different life
91 history traits in each sex, resulting in sex-specific selection pressures. For example, in the
92 Nearctic butterfly *Melitaea cinxia*, wing aspect ratio only correlates with dispersal in females,
93 as males experience additional selection pressures that counteract selection for dispersal
94 wing phenotypes (Breuker et al. 2007). Sex-specific behaviours can impact wing aspect ratio
95 and size, but differences in life histories, even across closely related species, could also
96 have large impacts on the strength and direction of these effects (Cespedes et al. 2015;
97 Chazot et al. 2016).

98

99 Another important source of phenotypic variation in insect wings is the physical environment
100 they inhabit throughout their range. Air pressure decreases with altitude, which in turn
101 reduces lift forces required for flight. To compensate for this, insects may increase wing area
102 relative to body size to reduce the velocity necessary to sustain flight (Dudley 2002; Dillon et
103 al. 2018). Wing aspect ratio in *Drosophila melanogaster* has been observed to vary
104 adaptively across latitudes and altitudes, with wings getting rounder and larger in montane
105 habitats, possibly to maintain flight function in lower air pressures (Stalker and Carson 1948;
106 Pitchers et al. 2012; Klepsatel et al. 2014).

107

108 In butterflies, high aspect ratios, i.e. long and narrow wings, reduce drag caused by wing tip
109 vortices, thus lowering the energy required for flight and promoting gliding for longer
110 distances (Le Roy et al. 2019). Variation in wing phenotypes can occur at the microhabitat
111 level, for example *Morpho* butterfly clades in the understory have rounder wings than

112 canopy-specialist clades, presumably for increased manoeuvrability (Chazot et al. 2016). An
113 extreme case of environmental effects on wing morphology can be found in Lepidoptera
114 inhabiting the windy, barren highlands of the Andes, where an interaction between
115 behavioural sex differences and extreme climatic conditions have led to flightlessness in
116 females of several species (Pyrz et al. 2004).

117

118 *Heliconius* is a genus of Neotropical butterflies that has been studied for over two centuries
119 with a well resolved phylogeny (Kozak et al. 2015, 2018). It represents a striking case of
120 Müllerian mimicry, with co-occurring subspecies sharing warning wing colour patterns to
121 avoid predators and leading to multi-species mimicry rings across South America (Merrill et
122 al. 2015). Wing aspect ratio and size are part of the mimetic signal (Jones et al. 2013; Mérot
123 et al. 2016; Rossato et al. 2018a). Wing morphology is involved in many aspects of
124 *Heliconius* biology other than mimicry, such as mating or flight mode, but these have been
125 less well studied (Rodrigues and Moreira 2004; Srygley 2004b; Mendoza-Cuenca and
126 Macías-Ordóñez 2010). As the only butterflies that pollen-feed, their long life-spans and
127 enlarged brains allow them to memorise foraging transects that are repeated daily following
128 a short dispersal post-emergence phase of up to 1.5 km (Cook et al. 1976; Jiggins 2016).

129

130 Larval gregariousness has evolved independently three times across the phylogeny, with
131 some species laying clutches of up to 200 eggs, while others lay eggs singly and larvae are
132 often cannibalistic (Beltrán et al. 2007). Gregarious *Heliconius* species would be predicted to
133 have larger-sized females to carry the enlarged egg load, as is the case with most
134 Lepidoptera (Allen et al. 2011). Another striking life history trait is pupal-mating, which is only
135 found in one of the two major clades (hereafter the “erato clade”), having arisen following the
136 most basal split in the *Heliconius* phylogeny. This mating strategy involves males copulating
137 with females as they emerge from the pupal case (Deinert et al. 1994; Beltrán et al. 2007).
138 Pupal-mating leads to a whole suite of distinct selection pressures but these are hard to
139 tease apart from the effects of phylogeny due to its single origin (Beltrán et al. 2007;

140 Thurman et al. 2018). Further ecological differences could arise from adaptation to altitude.
141 Some species are relatively high-altitude specialists, such as *H. telesiphe* and *H. hierax*
142 found above 1000m, whilst others range widely, such as *H. melpomene* and *H. erato*, which
143 can be found from 0 to 1800 m above sea-level (Rosser et al. 2015; Jiggins 2016). Potential
144 adaptations to altitude are yet to be explored.

145

146 The wide range of environments that *Heliconius* species inhabit, together with their diverse
147 natural history and well-resolved phylogeny make them a good study system for teasing
148 apart the selective forces driving wing phenotype (Merrill et al. 2015; Jiggins 2016). Here we
149 examine variation in wing aspect ratio and size across 13 species that span most of the
150 geographical range of the *Heliconius* genus. First, we photographed thousands of wings
151 collected by many *Heliconius* researchers since the 1990s from wild populations across
152 South and Central America, covering a 2100 m elevation range (Fig. 1 A). Wing dimensions
153 for 3515 individuals, obtained with an automated pipeline and standardised images, were
154 then used to address the following questions. (1) Are there size and aspect ratio sexual
155 dimorphisms, and if so, do they correlate with known life-history traits? (2) To what extent
156 are wing aspect ratio and size variation explained by shared ancestry? (3) Are wing aspect
157 ratio and size affected by the elevations species inhabit?

158 *Methods*

159 **STUDY COLLECTION**

160 The wild specimens studied here were collected using hand nets between 1998 and 2018 in
161 313 localities across Panama, Colombia, Ecuador, French Guiana, Suriname, and Peru (Fig.
162 1 A), and stored in the Department of Zoology, University of Cambridge (Earthcape
163 database). Collection altitudes ranged from sea level to 2100m above sea level (Fig 1 A).
164 Detached wings were photographed dorsally and ventrally with a DSLR camera with a 100
165 mm macro lens in standardised conditions. All the images are available in the public
166 repository Zenodo (<https://zenodo.org/communities/butterfly/>) and full records with data are
167 stored in the EarthCape database (<https://heliconius.ecdb.io>).

168

169 **WING MEASUREMENTS**

170 Damage to wings was manually scored in all the images and damaged specimens were
171 excluded from our analyses. To obtain wing measurements from the images, we developed
172 custom scripts for Fiji (Schindelin et al., 2012), to automatically crop, extract the right or left
173 forewing, and perform particle size analysis (Fig. 1 B). Butterflies predominantly use their
174 forewings for flight (Wootton 2002; Le Roy et al. 2019) and hindwings tend to be more
175 damaged in *Heliconius* due to in-flight predation and fragile structure, thus we only include
176 forewings here. Forewing and hindwing areas are tightly correlated in this genus (Strauss,
177 1990). For wing area, we obtained total wing area (in mm², hereafter “size”).

178

179 For examining wing aspect ratio, the custom scripts first fitted an ellipse to the forewings and
180 measured the length of the longest axis and the length of the axis at 90 degrees to the
181 former (Fig. 1 C). Aspect ratio corresponds to the length of the major axis divided by the
182 length of the minor axis, hereafter “aspect ratio” (Fig. 1 C). The data were checked for visual
183 outliers on scatter-plots, which were examined, and removed from the analyses if the wing
184 extraction pipeline had failed.

185

186 **STATISTICAL ANALYSES**

187 All analyses were run in R V2.13 (R Development Core Team 2011) and graphics were
188 generated with the package *ggplot2* (Ginestet 2011). Packages are specified below. All R
189 scripts can be found in the public repository Zenodo (Zenodo: TBC), including custom Fiji
190 scripts for wing image analysis. Species and sexes mean trait values were calculated for the
191 13 *Heliconius* species in our study. Each species had more than 30 individuals and all
192 individuals had accurate locality and altitude data (S.I.: Table S1), resulting in a dataset of
193 3515 individuals.

194

195 *Sexual dimorphism across species*

196 Sexual dimorphism in wing area and aspect ratio was estimated as the female increase in
197 mean wing area and aspect ratio with respect to males, thus negative values represent
198 larger trait values in males, while positive values represent larger trait values in females.
199 Pairwise t-tests were used to estimate the significance of sexual size/shape dimorphism in
200 each species.

201

202 We modelled variation in wing area and aspect ratio sexual dimorphism across species with
203 ordinary least squares (OLS) linear regressions, implemented in the 'lm' function. For
204 models of sexual wing area and aspect ratio sexual dimorphism, predictor variables initially
205 included larval gregariousness of the species (gregarious or solitary, as classified in Beltrán
206 et al. 2007), mating strategy (pupal-mating vs. adult-mating clade), species mean wing
207 aspect ratio and area, and species wing aspect ratio or size sexual dimorphism
208 (respectively). Wing size sexual dimorphism had a marginally significant phylogenetic signal
209 (Abouheif $C_{\text{mean}}=0.25$, $p=0.05$), so we present the sexual size dimorphism model
210 incorporating phylogeny as correlation term in the Supplementary Information (S.I., Table S3
211 and Table S4). We used backward selection with Akaike Information Criterion corrected for
212 small sample sizes (AICc, Hurvich and Tsai 1989) where the best models had the lowest

213 AICc values, implemented with the package MuMin (Bartón 2018). We report the overall
214 variation explained by the fitted linear models (R^2) and the relative contributions of each
215 explanatory variable (partial R^2), estimated with the package *relaimpo* (Grömping 2006).

216

217 *Variation across species*

218 To test whether variation in wing aspect ratio and area across species was constrained by
219 shared ancestry, we calculated the phylogenetic signal index Abouheif's Cmean (Abouheif
220 1999) which is an autocorrelation metric suitable for datasets with a relatively low number of
221 species and that does not infer an underlying evolutionary model (Münkemüller et al. 2012).
222 Observed and expected distribution plots for phylogenetic signal estimates are shown in the
223 Supplementary Information and were computed with the package *adephylo* (Jombart and
224 Dray 2010). We used a pruned tree with the 13 species under study from the most recent
225 molecular *Heliconius* phylogeny (Kozak et al., 2015). We plotted centred trait means across
226 the phylogeny with the function `barplot.phylo4d()` from the package *phylosignal* (Keck et al.
227 2016). To test and visualise phylogenetic signal further, we built phylocorrelograms for each
228 trait with the function `phyloCorrelogram()` of the same package, which estimates Moran's I
229 autocorrelation across matrices with varying phylogenetic weights. Then, the degree of
230 correlation (Morans' I) in species trait values can be assessed as phylogenetic distance
231 increases (Keck et al. 2016).

232

233 To study variation in wing area and aspect ratio across species we took a phylogenetic
234 comparative approach. These methods assume that species-specific mean trait values are a
235 good representation of the true trait values of the species under study, in other words, that
236 the within-species variation is negligible compared to the across-species variation
237 (Garamszegi 2014). To test this, we first used an ANOVA approach, with species as a factor
238 explaining the variation of mean trait values. We then estimated within-species trait
239 repeatability, or intra-class correlation coefficient (ICC), with a linear mixed model approach.

240 This requires the grouping factor to be specified as a random effect, in this case species,
241 with a Gaussian distribution and 1000 parametric bootstraps to quantify uncertainty,
242 implemented with the function `rptGaussian()` in *rptR* package (Stoffel et al. 2017). By
243 specifying species as a random effect, the latter approach estimates the proportion of total
244 trait variance accounted for by differences between species. A trait with high repeatability
245 indicates that species-specific trait means are reliable estimates for further analyses (Stoffel
246 et al. 2017). We, nevertheless, accounted for within-species variation in the models
247 described below.

248

249 To test the effect of altitude on wing aspect ratio and size across species, we used a
250 phylogenetic generalised least squares (PGLS) approach. Species wing trait means may be
251 correlated due to shared ancestry (Freckleton et al. 2002; Chazot et al. 2016). Therefore, to
252 explore the effects of the environment on the traits under study, models that incorporate
253 expected correlation between species are required, such as PGLS. Although often ignored,
254 these models assume the presence of phylogenetic signal on the model residuals of the trait
255 under study (here wing aspect ratio or size) controlling for covariates that affect the trait
256 mean (allometry, sex ratio) , and not just phylogenetic signal on the species mean trait
257 values (Revell 2010; Garamszegi 2014). Thus, to check if this assumption was met we
258 estimated phylogenetic signal as described above (Keck et al. 2016) for the residuals of a
259 generalised least squares (GLS) of models that had wing aspect ratio or size as response
260 variables, and the size and aspect ratio (respectively) and sex ratio as explanatory variables,
261 to ensure this assumption of PGLS model was met. To visually inspect phylogenetic signal on
262 the residuals we obtained phylogenetic correlograms for these and centred trait residuals for
263 plotting across the phylogeny as detailed above for trait means (presented in the S.I., Fig.
264 S3 and Fig. S4 (Keck et al. 2016).

265

266 Significant phylogenetic signal was detected in mean wing size and in the residuals of both
267 traits, wing aspect ratio and area regression models (S.I., Fig. S4, Fig. S5), so we used

268 maximum log-likelihood PGLS regression models with the phylogenetic correlation fitted as
269 a correlation term, implemented with the `gls()` function from the *nlme* package (Pinheiro et al.
270 2007). We assumed a Brownian motion model of trait evolution for both traits, by which
271 variation across species accumulated along all the branches at a rate proportional to the
272 length of the branches (Freckleton et al. 2002). To select the most supported model given
273 the available data, i.e. one that improves model fit while penalising complexity, we used the
274 Akaike Information Criteria corrected for small sample sizes (AICc, Hurvich and Tsai 1989),
275 where the best models had the lowest AICc values, implemented with the package MuMin
276 (Bartón 2018). Maximal PGLS models included species mean altitude and distance from the
277 Equator (to control for potential latitudinal clines), sex ratio in our samples interacting with
278 either wing aspect ratio or wing size, to control for potential allometric and sexual
279 dimorphism relationships, which could be different among closely-related taxa (Outomuro
280 and Johansson 2017). Most species are found in the Andean mountains or the Amazonian
281 region near the Equator, so we did not have much power to examine variation with latitude in
282 wing aspect ratio and size across species, but we included distance from the Equator as an
283 explanatory variable in the PGLS models to account for it. Minimal PGLS models consisted
284 of the trait under study explained solely by its intercept, without any fixed effects. All model
285 selection tables can be found in the S.I. (Table S3, S5). Finally, we weighted PGLS
286 regressions to account for unequal trait variances and unbalanced sample sizes across
287 species (for sample sizes and standard errors of species' trait means see S.I. Table S1).
288 This was achieved by modifying the error structure of the model with combined variances
289 obtained with the function `varFixed()` and specified with the argument "weights" (Pinheiro et
290 al. 2007; Paradis 2012; Garamszegi 2014). In this study, 74.8% of the individuals were
291 collected in the last 10 years, thus we did not have power to detect any changes in wing
292 morphology across species potentially incurred by climate change (Fig. S1). Future studies
293 could focus on temporal changes in wing morphology in areas and species that have been
294 well sampled throughout the years.

296 *Variation within species*

297 We selected the two most abundant and geographically widespread species within our
298 dataset, *H. erato* (n=1685) and *H. melpomene* (n= 912) (S.I. Table S1), to examine variation
299 in wing area and aspect ratio within species. We modelled variation in size and aspect ratio
300 with ordinary least squares (OLS) linear regressions for each species, implemented in the
301 'lm' function. For all models, predictor variables initially included the terms altitude, distance
302 from the Equator, longitude, aspect ratio or wing area, and sex, as well as the plausible
303 interactions between them (Table S5). We then used step backward and forward selection
304 based on AIC with the function stepAIC(), from the MASS package (Ripley, 2011; Zhang,
305 2016) (full models and model selection tables in S.I. Table S5, S6).

306

307 *Results*

308 We obtained intact-wing measurements for 3515 individuals of 13 *Heliconius* species from
309 across the phylogeny and from over 350 localities (Fig. 1, Table S1). We have made all of
310 these wing images publicly available at the Zenodo repository.

311

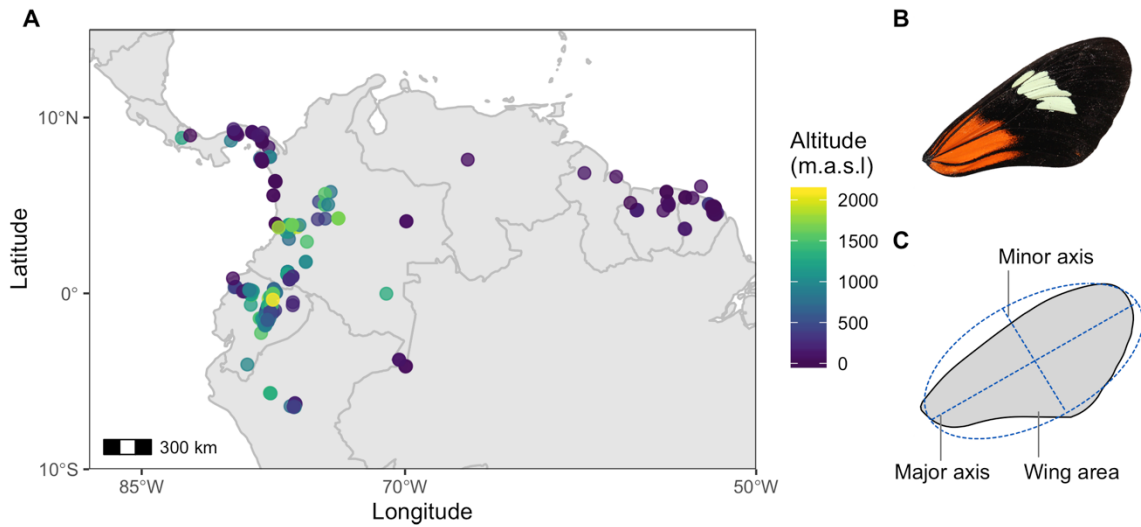
312 **SEXUAL DIMORPHISM**

313 Sexual dimorphism in wing area was found throughout the phylogeny, but in opposing
314 directions in different species (Fig. 2). Mean sizes were significantly or marginally
315 significantly different among sexes in nine species, all of which were represented by more
316 than 40 individuals (S.I., Table S2 for two sample T-test summary statistics), indicating that
317 the non-significant trends in other species probably reflect a lack of power caused by low
318 numbers of females typically collected in the wild (S.I., Table S1). The six species with
319 trends toward larger females have gregarious larvae (pink, Fig. 2), whereas the seven
320 species with trends toward larger males lay eggs singly (black, Fig. 2). Larval
321 gregariousness alone explained 69% of the total natural variation in sexual size dimorphism
322 across species (Table 1; Gaussian LM: $F_{1,11} = 27.2$, $P < 0.001$, $R^2 = 0.69$). There was a
323 marginally significant phylogenetic signal in sexual size dimorphism (Abouheif's
324 $C_{\text{mean}} = 0.24$, $P = 0.05$; S.I., Fig. S3), so we repeated the analysis accounting for phylogeny
325 and the results are presented in the Supplementary Information. This would be expected
326 from the evolutionary history of gregariousness, as it is present in all species of three
327 lineages that are well represented in our study (Beltrán et al. 2007). However, when
328 accounting for phylogenetic correlation in the model larval gregariousness remained a
329 significant predictor of size sexual dimorphism (S.I., Table S4).

330

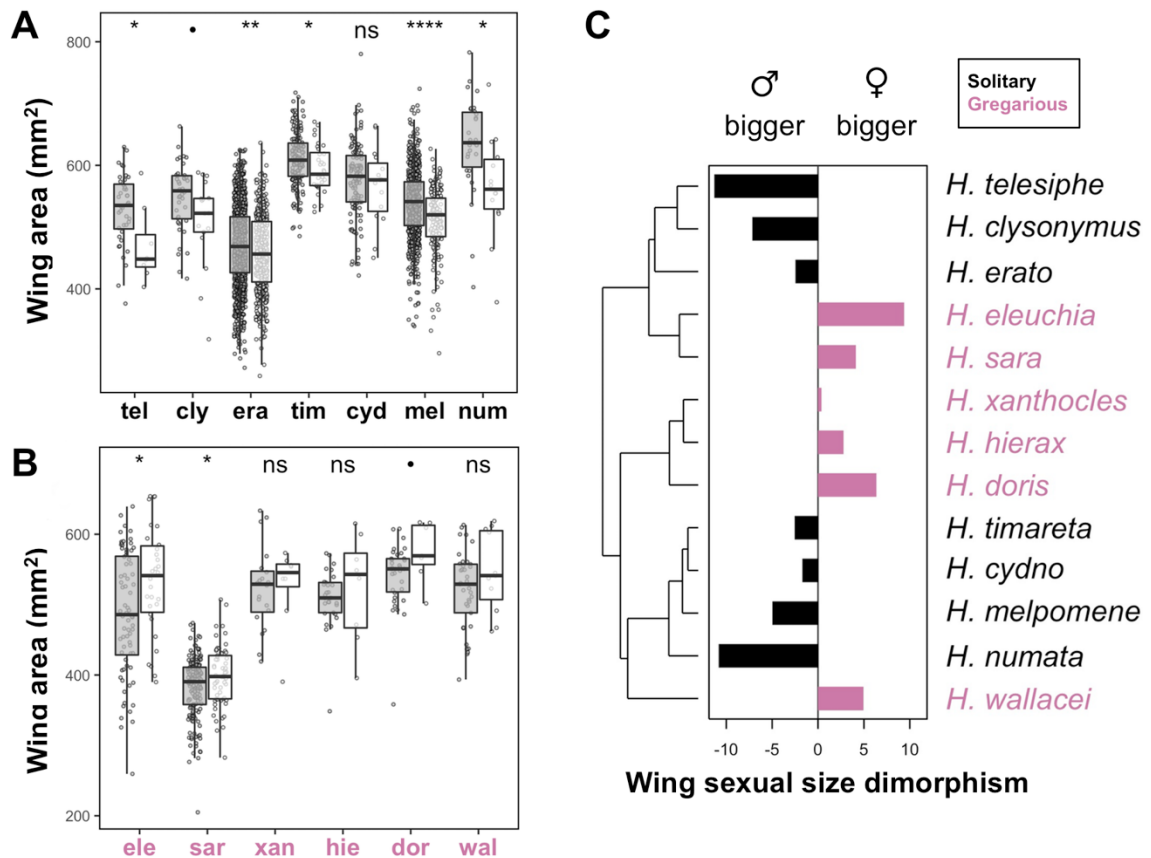
331 Sexual dimorphism in wing aspect ratio was found in three species (Fig. S4), *H. erato* and *H.*
332 *wallacei* had longer-winged males whereas the high-altitude specialist *H. eleuchia* had
333 longer-winged females (Table S2, T-test, *H. erato*: $t_{843} = 10.4$, $P < 0.0001$, *H. eleuchia*: $t_{49} = -2.3$,

334 $p < 0.05$, *H. wallacei*: $t_{19} = 2.2$, $P < 0.05$). Wing aspect ratio sexual dimorphism across species
335 could not be explained with the variables here studied and had no phylogenetic signal
336 (Abouheif's $C_{mean} = -0.02$, $P = 0.3$; S.I., Fig. S3).



337

338 **Figure 1.** Localities and forewing measurements. (A) Map of exact locations (n=313)
339 across South America from where the samples used for our analyses were collected.
340 Points are coloured by altitude. (B) Representative of a right forewing image of *H.*
341 *melpomene malleti*. (C) Measurements taken from each wing by fitting an ellipse with
342 Fiji custom scripts.
343



344
 345
 346
 347
 348
 349
 350
 351
 352
 353
 354
 355

Figure 2. Sexual wing area dimorphism across species and the phylogeny. (A) Wing size differences between males (grey) and females (white) of the seven single egg-laying species and (B) the six gregarious species in this study. Error bars represent 95% confidence intervals of the means. Stars represent significance levels of two sample t-tests between female and male wing areas for each species ($\bullet < 0.1$, $* < 0.05$, $** < 0.01$, $*** < 0.001$), for full t-tests output see Table S1. (C) Bar plot represents sexual size dimorphism calculated as percentage difference in female vs. male size (positive means bigger females, right panel). Species with gregarious larvae are coloured in pink, and those with solitary larvae are coloured in black.

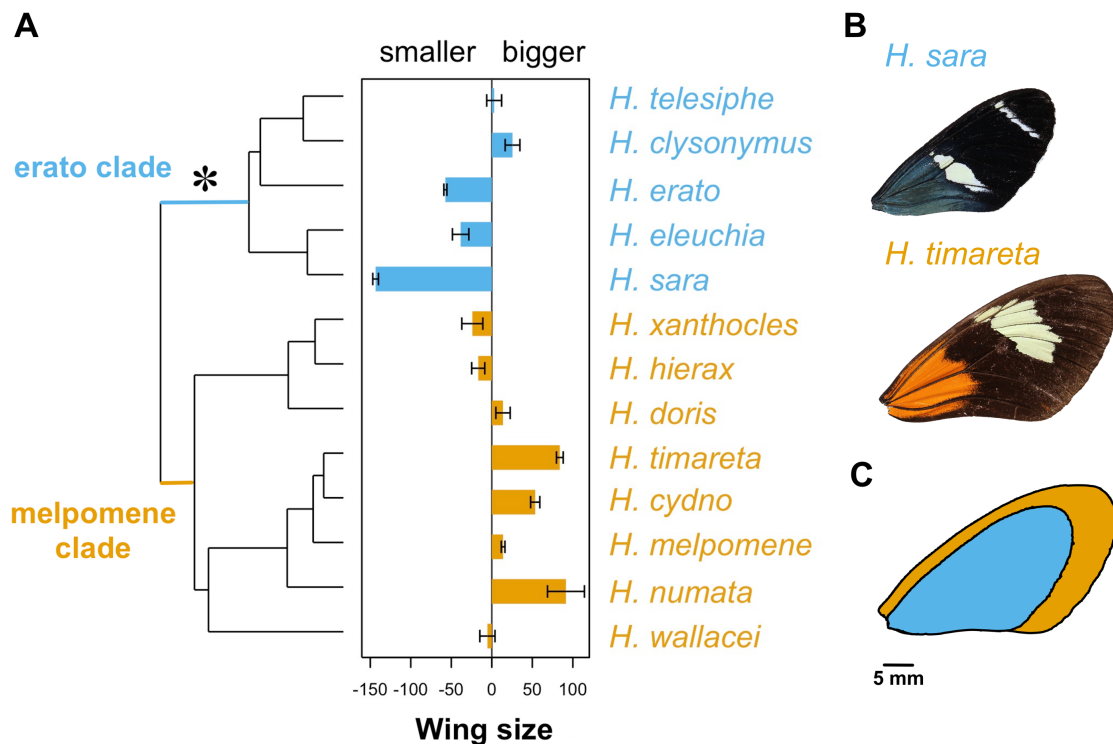
356 PHYLOGENETIC SIGNAL

357 The 13 *Heliconius* species studied differed significantly in wing area and aspect ratio
 358 (ANOVA, Aspect ratio: $F_{12, 3502} = 228.4$, $P < 0.0001$, Area: $F_{12, 3502} = 216.4$, $P < 0.0001$;
 359 Tukey-adjusted comparisons S.I. Fig. S2). We estimated within-species trait repeatability to
 360 assess their reliability as species mean estimates for phylogenetic analyses. Wing aspect
 361 ratio had higher intra-class repeatability than wing area, with 74% and 48% of the total
 362 aspect ratio and size variance explained by differences between species, respectively

363 (Aspect ratio: $R=0.74$, $S.E.=0.09$, $P<0.0001$; Size: $R=0.48$, $S.E.=0.1$, $P<0.0001$). We
364 estimated intra-class repeatability for males and females separately to remove the potential
365 effect of size sexual dimorphism on trait variation, and male size repeatability remained
366 much lower than male wing aspect ratio repeatability (Male aspect ratio: $R=0.75$, $S.E.=0.08$,
367 $P<0.0001$; Male Size: $R=0.53$, $S.E.=0.1$, $P<0.0001$). Females had the same wing aspect
368 ratio repeatability as males, whereas wing size repeatability was lower for females probably
369 due to smaller sample sizes (Female aspect ratio: $R=0.75$, $S.E.=0.05$ $P<0.0001$; Female
370 Size: $R=0.44$, $S.E.=0.1$, $P<0.0001$).

371

372 Mean wing aspect ratio showed no phylogenetic signal (Abouheif's $C_{mean}=0.15$, $P=0.1$;
373 S.I.: Fig. S3, Fig. S5 B), in other words closely-related species were not more similar to each
374 other than to distant ones. In contrast, mean wing area showed a strong phylogenetic signal,
375 by which phylogenetically closely-related species were more likely to have similar wing
376 areas (Fig. 3, Abouheif's $C_{mean}=0.33$, $P=0.01$; S.I.: Fig. S3, Fig. S6 A, B). Wing areas of
377 species in the melpomene clade were on average 14.8% larger than those of species in the
378 erato clade, with *H. timareta* being 64% larger than *H. sara* (Fig. 3, *H. timareta*: mean=606.6
379 mm^2 , $s.e.=3.1$; *H. sara*: mean=387 mm^2 , $s.e.=2.9$). Nevertheless, when controlling for sex
380 ratios and allometry on the traits under study, wing aspect ratio and size, the residuals of
381 both traits show a strong phylogenetic signal (S.I.: Fig. S5/6 AC; Aspect ratio residuals:
382 Abouheif's $C_{mean}=0.42$, $P<0.001$; Fig. S3 A, C- Size residuals: Abouheif's $C_{mean}=0.44$,
383 $P<0.001$). These results support the use of phylogenetic models to study variation in wing
384 aspect ratio and size across species.

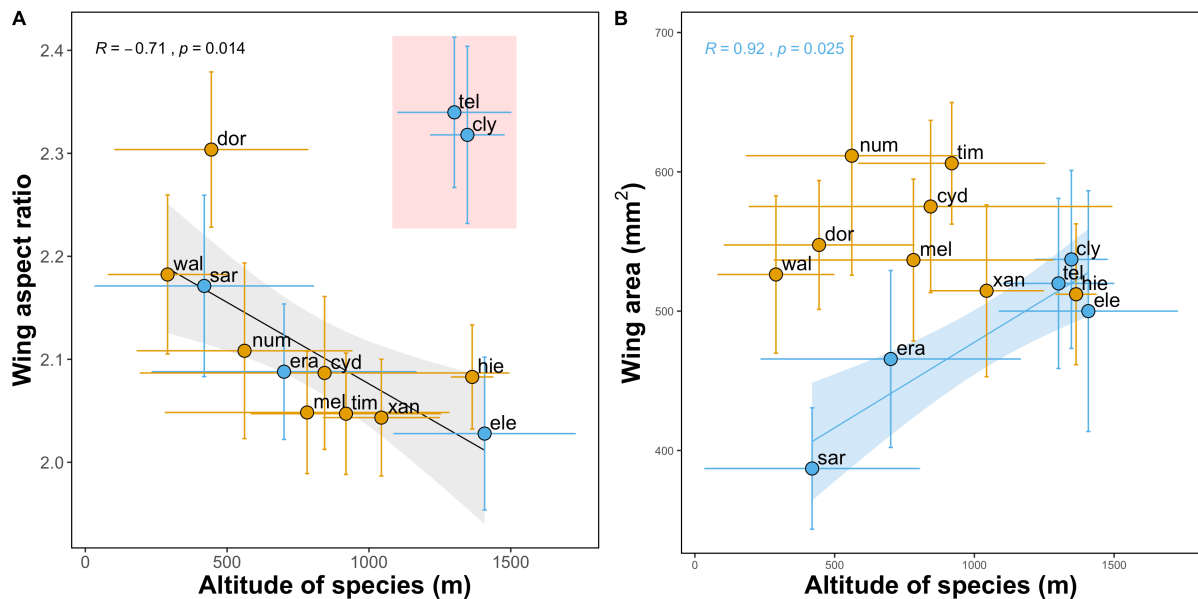


385 **Figure 3.** Male wing area differences across the phylogeny. (A) Bar plot represents
 386 centred mean wing area per species (positive values represent species with bigger
 387 wings than the average *Heliconius* wing). Wing area, x-axis, is the difference in wing
 388 area from the mean (in mm²). Error bars represent standard errors. The star
 389 represents the origin of pupal-mating. Species from the erato clade are in blue, and
 390 those from the melpomene clade are in orange. (B) Representatives of *H. timareta*
 391 and *H. sara* closest to the mean wing area of the species are shown (606.25 mm²
 392 and 386.6 mm², respectively). (C) Images from (B) superimposed to compare
 393 visually the mean size difference between the two species.
 394
 395

396 PATTERNS ACROSS SPECIES AND ALTITUDES

397 Species mean altitude had an effect on wing area and aspect ratio (Table 1). Species wings
 398 got rounder, i.e. lower aspect ratios, with increasing altitudes both when accounting for fixed
 399 effects and the phylogeny (Table 1, full model Table S4). These patterns were also evident
 400 when examining raw mean wing aspect ratios (Fig. 4A, Gaussian LM: $F_{1,9} = 5.37$, $P < 0.05$,
 401 $R^2=0.30$), except in the *H. telesiphe* and *H. clysonymus* highlands clade, which showed
 402 significant phylogenetic autocorrelation (Moran's I index: *H. clysonymus* 0.53, *H. telesiphe*
 403 0.49). Species wings got larger with elevation (Table 1, full model Table S4). Without
 404 accounting for phylogeny or any fixed effect this is only evident in the erato clade, where

405 high altitude species were bigger than their lowland sister species (Fig. 4B, blue, Gaussian
 406 LM: $F_{1,10} = 17.1$, $R^2 = 0.80$, $p = 0.03$). However, when assessing individuals from all species
 407 together, it becomes clear that larger individuals of both clades tend to be found at higher
 408 altitudes (Fig. S8). Both wing size and wing aspect ratio were also significantly correlated
 409 with distance from the Equator, and wing aspect ratio was affected by species sex ratio too
 410 (S.I. Table S4).



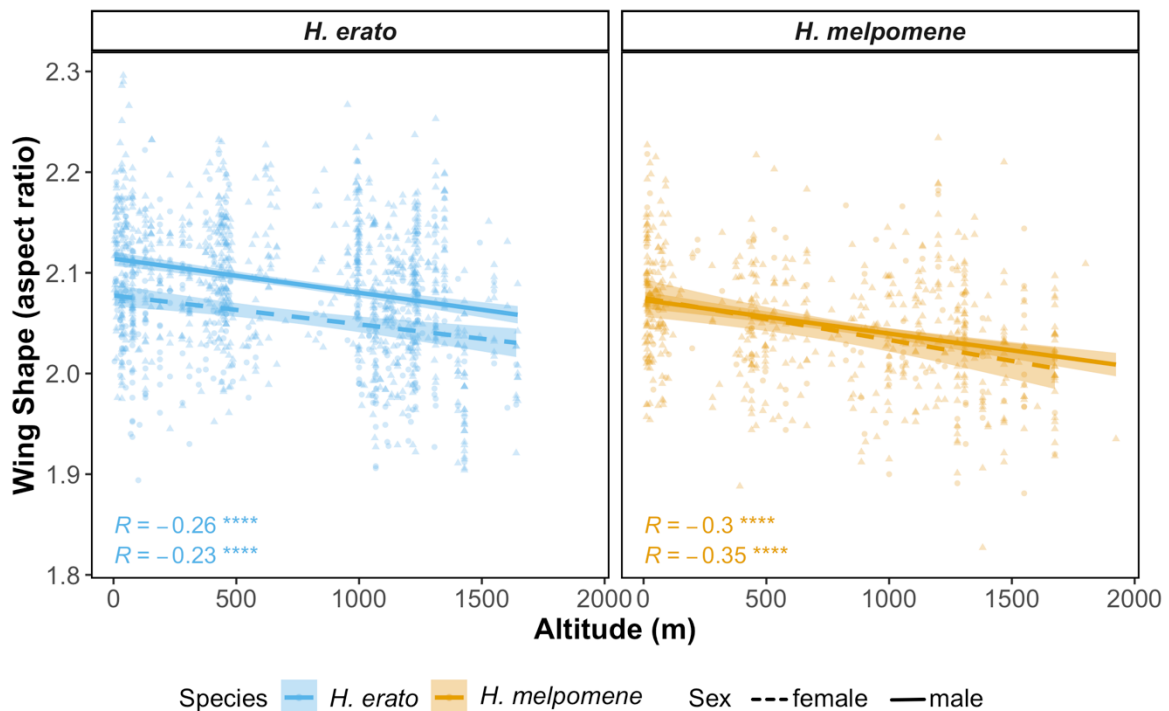
411
 412
 413 **Figure 4.** Species variation in wing aspect ratio (A) and wing area (B). Plots show
 414 the effect of altitude (meters above sea level) on wing aspect ratio (major axis/minor
 415 axis, higher values represent longer wings) and wing area (mm²). Points represent
 416 species mean raw values per species. Horizontal and vertical lines show standard
 417 error for species mean altitude and mean trait, respectively. Lines show best linear fit
 418 and are coloured by clade when clade was a significant predictor (blue: erato clade,
 419 orange: melpomene clade). Shaded areas show confidence bands at 1 standard
 420 error. The point labels correspond to the first three characters of the following
 421 *Heliconius* species: *H. telesiphe*, *H. clysonymus*, *H. erato*, *H. eleuchia*, *H. sara*, *H.*
 422 *doris*, *H. xanthocles*, *H. hierax*, am*H. wallacei*, *H. numata*, *H. melpomene*, *H.*
 423 *timareta*, *H. cydno*. Two species, *H. telesiphe* and *H. clysonymus*, showed high
 424 levels of phylogenetic autocorrelation (Fig. S7) and were thus excluded from the
 425 linear model plotted (but not from the main analyses where phylogeny is accounted
 426 for).

427

428 PATTERNS WITHIN SPECIES AND ACROSS ALTITUDES

429 Wings got rounder (lower aspect ratio) with increasing altitude in *H. erato* and *H. melpomene*
 430 (Fig. 5. *H. erato*: Gaussian LM: $F_{6, 1296} = 32.7$, $P < 0.001$, $R^2 = 0.13$; *H. melpomene*: Gaussian

431 LM: $F_{6, 673} = 20.1$, $P < 0.001$, $R^2=0.14$). Individual altitude was the strongest predictor of wing
 432 aspect ratio for both species, with sex and wing area being second best in *H. erato* and *H.*
 433 *melpomene*, respectively (Table S6, Fig. S13 A and B, Fig. 5). Conversely, the relative
 434 importance of explanatory variables of wing area varied for each species (Table S6, Fig. S13
 435 A and B, Fig. 5), and the *H. erato* model explained less of the overall variation in wing area
 436 (Fig. S11, *H. erato*: Gaussian LM: $F_{7, 1295} = 9.36$, $P < 0.001$, $R^2=0.04$, *H. melpomene*:
 437 Gaussian LM: $F_{7, 672} = 23.06$, $P < 0.001$, $R^2=0.18$). Wing area in *H. erato* was correlated with
 438 allometric factors interacting with altitude, whereas wing area in *H. melpomene* was
 439 correlated with distance from the Equator (Table S6, Fig. S10 and S13 C and D). Wing area
 440 and aspect ratio differed among co-mimicking races of *H. erato* and *H. melpomene*, despite
 441 inhabiting the same geographic areas (Fig. S12).



442

443 **Figure 5.** Within-species variation in wing aspect ratio across altitudes in *H. erato*
 444 (blue) and *H. melpomene* (orange), females (triangles, dotted line) and males
 445 (circles, solid line). Lines show best linear fit and are colored by species. Shaded
 446 areas show confidence bands at 1 standard error. Pearson correlation coefficients
 447 and p-values are shown for each regression plotted.

448

449

450 *Discussion*

451 The fascination for butterfly wing colouration has stimulated many generations of research
452 and *Heliconius* wing patterns have proven to be excellent study systems for understanding
453 evolution and speciation. Here we have extended this research by examining wing shape
454 and size variation among more than 3500 individual butterflies, across sexes, clades, and
455 altitudes in 13 species of *Heliconius* butterflies. We have shown that a large proportion of
456 female biased sexual size dimorphism can be explained by the evolution of larval
457 gregariousness, and that male biased sexual size dimorphism is present only in species that
458 lay eggs singly, regardless of their mating strategy. For the first time in this system, we
459 describe wing morphological variation across environmental clines, with species and
460 populations found at higher altitudes consistently having rounder wings. Here we
461 demonstrate that *Heliconius* wing area and aspect ratio are potentially shaped by a plethora
462 of behavioural and environmental selection pressures, in addition to those imposed by
463 Müllerian mimicry.

464

465 **WING ASPECT RATIO VARIATION**

466 Wing aspect ratio in butterflies and other flying animals determines flight mode and speed
467 (Farney and Fleharty 1969; Buler et al. 2017), and is therefore predicted to vary with life-
468 history requirements across sexes and species. Despite being a simple descriptor of wing
469 shape, aspect ratio has been demonstrated to correlate functionally with gliding efficiency in
470 butterflies by increasing lift-to-drag ratios (Ortega Ancel et al. 2017; Le Roy et al. 2019).
471 Long wings are generally associated with faster gliding flying, whereas round wings with low
472 aspect ratio values favour slow but more manoeuvrable flight motions (Betts and Wootton
473 1988; Chai and Srygley 1990; Chazot et al. 2016; Le Roy et al. 2019). For instance,
474 monarch butterfly populations with longer migrations have more elongated wings than
475 resident populations (Satterfield and Davis 2014), and males of *Morpho* species that dwell in
476 the canopy also have higher aspect ratios to glide faster through open areas (DeVries et al.

477 2010). In contrast, female *Morpho* butterflies tend to have rounder wings, and aspect ratio
478 sex differences are stronger in species with colour dimorphism, as varying crypsis may
479 require specific flight behaviours (Chazot et al. 2016).

480

481 *Heliconius* are not notoriously sexually dimorphic especially when compared to other
482 butterflies such as *Morpho* (Chazot et al. 2016; Jiggins 2016). However, there are important
483 behavioural differences between the sexes. Females are thought to have different flight
484 habits, as they spend much of their time looking for specific host plants for oviposition
485 (Dell'Aglio et al. 2016), or precisely laying eggs on suitable plants, while males tend to patrol
486 open areas searching for receptive females and visit flowers more often (Joron 2005; Jiggins
487 2016). Thus, it might be predicted that females should have lower aspect ratios, i.e. rounder
488 wings, than males (Jones et al. 2013). However, we only found three species with
489 significant, but opposing, sexually dimorphic wing aspect ratios. The wings of males in *H.*
490 *erato* were longer than the wings in females, whereas male *H. eleuchia* and *H. wallacei* had
491 rounder wings than those of females (S.I. Fig. S3). *Heliconius* wing shape sex differences
492 may require multivariate descriptors of wing morphology and/or analysis of the hindwings,
493 which possess the pheromone-dispersing androconial patch in males (Jones et al. 2013;
494 Mérot et al. 2013, 2016). In addition, the relatively low collection numbers of female
495 *Heliconius* could hinder the detection of subtle wing aspect ratio differences across the
496 sexes.

497

498 Sexual selection has long been known to affect wing colour pattern in *Heliconius*, as it is
499 used for mate recognition and choice (Merrill et al. 2012). More recently, wing aspect ratio
500 has been shown to be part of the mimetic warning signal in *Heliconius* and their co-mimics
501 (Jones et al. 2013), as it determines flight motion and defines the overall appearance of the
502 butterfly (Srygley 1994, 2004a). For instance, wing aspect ratios between two different
503 morphs of *H. numata* differed consistently across their overlapping ranges, in parallel with
504 their respective and distantly related *Melipotis* co-mimics (Jones et al. 2013). Within-morph

505 wing aspect ratio variation was observed across the altitudinal range of *H. timareta* in Peru
506 (Mérot et al. 2016), and in the *Heliconius* postman mimicry ring in Brazil significant across-
507 species wing aspect ratio differences were also found (Rossato et al. 2018a). These studies
508 highlight that while it is clear that colour pattern and, to some extent, flight are important for
509 mimicry in *Heliconius*, wing aspect ratio is also subject to other selection pressures (Mérot et
510 al. 2016; Rossato et al. 2018b).

511

512 We found that species inhabiting higher altitudes tend have rounder wings, after accounting
513 for phylogeny, sample size and intra-specific variance (Fig. 4 A), except in the *H. telesiphe* –
514 *H. clysonymus* clade. The latter species may require morphometric analyses of wing tip
515 shape alone, as the overall wing morphology differs significantly from the rest of the
516 *Heliconius* species here studied (Fig. S7). Interestingly, these patterns were maintained
517 within-species, with high-altitude populations of *H. erato* and *H. melpomene* having lower
518 aspect ratios (Fig. 5). Furthermore, altitude was the best predictor of wing aspect ratio in
519 both species (Fig. S13). Rounder wings aid manoeuvrability and are associated with slower
520 flight in butterflies (Berwaerts et al. 2002; Le Roy et al. 2019) and slower flights are generally
521 associated with a decrease in ambient temperature (Gilchrist et al. 2000). In addition, air
522 pressure, which directly reduces lift forces required to offset body weight during flight (Dillon
523 2006), decreases approximately 12% across the mean altitudinal range of the species here
524 studied. Thus, the rounder wings in high altitude *Heliconius* species and populations may aid
525 flying in dense cloud forests, where increased manoeuvrability could be beneficial, or
526 compensating for lower air pressure at higher altitude.

527

528 **WING AREA VARIATION**

529 Wing area showed significant sexual dimorphism in more than half of the species studied
530 here, but some species had larger males and others larger females (Fig. 2). In most
531 butterflies, females are overall larger than males, presumably because fecundity gains of
532 increased body size are greater for females (Allen et al. 2011). Larger wings are required to

533 carry larger and heavier bodies, and so Lepidoptera females also tend to have larger wings
534 (Allen et al. 2011; Le Roy et al. 2019). Indeed, in this study the *Heliconius* species with
535 larger-winged females were those that lay eggs in large clutches and that have highly
536 gregarious larvae (Fig. 2 , Beltrán et al. 2007). A recent study on two species not included
537 here reported wing size dimorphism with larger females in the gregarious *H. eratosignis*
538 *ucayalensis* and larger males in the single-egg layer *H. demeter joroni* (Rosser et al. 2019).
539 Thus, females of these species are likely investing more resources in fecundity than males,
540 which leads to larger body and wing sizes that allow them to carry and lay eggs in clutches
541 throughout adulthood. Larval development time correlates with adult size in *H. erato*
542 (Rodrigues and Moreira 2002) and growth rates seem to be the same across sexes, at least
543 in the gregarious *H. charithonia* (Kemp 2019), so we hypothesize that females take longer to
544 develop in gregarious species. Selection for larger females is generally constrained by a
545 trade-off between the benefits of increased fecundity at the adult stage and the higher
546 predation risk at the larval stage associated with longer development times (Allen et al.
547 2011). This constraint might be alleviated in the unpalatable larvae of *Heliconius*, as bigger
548 larval and adult size could increase the strength of the warning toxic signal to predators
549 (Jiggins 2016).

550

551 An extensive survey identified that only six percent of lepidopteran species exhibit male-
552 biased sexual size dimorphism, and that these patterns were generally explained by male-
553 male competition (i.e. intrasexual selection), in which larger males had a competitive
554 advantage (Stillwell et al. 2010; Allen et al. 2011). In contrast, nearly half of the *Heliconius*
555 species studied here have male-biased sexual size dimorphism, and all of these lay eggs
556 singly and have solitary larvae (Fig. 2). Male-male competition is high for *Heliconius* species,
557 as females rarely re-mate despite their very long reproductive life-spans (Merrill et al. 2015).
558 In addition, large reproductive investments in the form of nuptial gifts from males can, in
559 principle, explain male-biased sexual size dimorphisms, as is the case in the polyandrous
560 butterfly *Pieris napi* whose male spermatophore contains the amount of nitrogen equivalent

561 to 70 eggs (Karlsson 1998; Allen et al. 2011). Male *Heliconius* spermatophores are not only
562 nutrient-rich, but also loaded with anti-aphrodisiac pheromones that prevent re-mating of
563 fertilised females (Schulz et al. 2008; Merrill et al. 2015). Therefore, it seems likely that in
564 species that lay eggs singly, sexual selection favouring larger males exceeds selection
565 pressures for the large female size needed to carry multiple mature eggs. To our knowledge,
566 *Heliconius* is the first example of a butterfly genus in which both female- and male-biased
567 size dimorphism are found and can be explained by contrasting reproductive strategies.

568
569 We found a strong phylogenetic signal for wing area, with species from the erato clade being
570 on average 12% smaller than those in the melpomene clade (Fig. 3). There are many
571 ecological factors that could explain this pattern, and all could have contributing effects that
572 are hard to disentangle (Fig. 3). Firstly, the erato clade is characterised by facultative pupal-
573 mating (Beltrán et al. 2007; Jiggins 2016), by which males fight for pupae, guard them, and
574 mate with females as they are emerging from the pupal case (Deinert et al. 1994; Jiggins
575 2016). Smaller males have been shown to outcompete others for a spot on the female pupal
576 case and more successfully inseminate emerging females compared to larger, less agile
577 males (Deinert et al. 1994), which would remove the potential choice of females for larger
578 males. Secondly, pupal-mating seems to have far-reaching impacts on species life-histories
579 (Boggs 1981). Species in the melpomene or adult-mating clade are polyandrous, which
580 leads to selection favouring large spermatophores (Boggs 1981) to provide mated females
581 with abundant nutritional resources and defences that prevent them from re-mating with
582 other males (Cardoso et al. 2009; Cardoso and Silva 2015). This could decrease selection
583 pressure for larger males in the pupal-mating clade, as nuptial gifts need not be so large or
584 nutrient/defence rich, leading to smaller male and female offspring. However, the single
585 origin of pupal-mating in *Heliconius* (Fig. 2) makes it challenging to infer the impacts of this
586 mating strategy on wing morphology, as the behaviour is confounded by phylogeny.

587

588 Wing area across species positively correlated with altitude in the erato clade (Fig. 4B), but
589 no clear pattern was found for the melpomene clade species here studied. In contrast, wing
590 area variation within-species (*H. erato* and *H. melpomene*) was more correlated with
591 geography (distance to Equator, longitude) and allometry than with altitude (Fig. S10).
592 Nevertheless, high-altitude populations of *H. melpomene* were slightly bigger than their
593 lowland conspecifics, whereas *H. erato* did not change (S.I., Fig. S13). Two major
594 environmental factors are known to affect insect size across altitudinal clines. One is
595 temperature, such that at lower temperatures, development times are longer and insects
596 grow larger (Chown and Gaston 2010). This perhaps explains cases of Bergmann's rule
597 among ectotherms, where larger species are found in colder climates (Shelomi 2012;
598 Classen et al. 2017). In the geographical range here studied (Fig. 1), we predict
599 temperatures to vary more dramatically along elevational gradients than latitudinal gradients
600 (García-Robledo et al. 2016). We found some evidence for species being bigger with
601 increasing latitudes when accounting for phylogeny and allometry (Table S4), in accordance
602 with Bergmann's rule, but more species at the extremes of the ranges are needed to clarify
603 this (Fig. S7).

604

605 Wing beat frequency tends to be lower at low temperatures, so larger wings are required to
606 compensate and gain the extra lift required for flight, as seen in *Drosophila robusta*
607 (Azevedo et al. 2006; Dillon 2006). A second factor likely to contribute to altitude related
608 differences in wing area is air pressure changes and the correlated lower oxygen availability,
609 which affects flight motion and kinematics as well as many physiological processes. High-
610 altitude insects can minimise the impacts of lower air pressure by having larger wings,
611 because this lowers the velocity required to induce flight (Dudley 2002).

612

613 **HERITABILITY**

614 Our study demonstrates that multiple selective forces may be affecting *Heliconius* wing area
615 and aspect ratio. However, this raises the question of how plastic these traits are in the wild.

616 In *Drosophila*, the genetic architecture of wing aspect ratio appears to be complex (Gilchrist
617 and Partridge 2001), and is independent of that of wing area (Carreira et al. 2011). Within-
618 species variability of wing area halved when flies were reared in controlled conditions
619 compared to wild populations whereas wing shape variability remained the same, but both
620 traits had a detectable and strong heritable component (Bitner-Mathé and Klaczko 1999;
621 Klaczko 1999). In this study we found that 74% of the variation in wing aspect ratio could be
622 explained by species identity, in contrast to 48% of the variation in wing area. This high and
623 moderate intra-class repeatability is indicative of heritable traits (Nakagawa and Schielzeth
624 2013). The fact that closely related species are more likely to have similar wing
625 morphologies, i.e. phylogenetic signal, is also indicative of species-level heritability (Queiroz
626 and Ashton 2004).

627

628 In insects wing shape is functionally more constrained than wing size. For example, genetic
629 manipulations of wing shape in *Drosophila melanogaster* have shown that even subtle
630 changes can have huge biomechanic impacts (Ray et al. 2016), whereas wing/body size
631 differences may impact fecundity more than survival. Here we find size differences between
632 sexes that can be explained by reproductive strategy, and are likely to be genetically
633 controlled as most sexual dimorphisms are (Allen et al. 2011). The patterns of variation in
634 size across altitudes or latitudes are often not due to phenotypic plasticity alone, as many
635 studies have shown their retention when populations are reared in common-garden
636 conditions (Chown and Gaston 2010). In Monarch butterflies, for example, common-garden
637 reared individuals from wild populations that had different migratory habits showed a strong
638 genetic component for both wing aspect ratio and size (Altizer and Davis 2010).

639

640 We have shown that different selection pressures may be shaping the evolution of wing
641 morphology in *Heliconius* and that the strength of these varies across sexes and
642 environmental clines. Interestingly some of these patterns are maintained at the intra-
643 specific level, with high-altitude populations of *H. erato* and *H. melpomene* having rounder

644 wings (Fig. 5), thus potentially adapting locally to the environment in the same way that
645 species of this genus have adapted to altitude over longer evolutionary timescales (Fig. 4).
646 Future work should assess the adaptive significance, plasticity, and heritability of these traits
647 with common-garden rearing and physiological assays in controlled conditions.

648

649 **CONCLUSIONS**

650 Here we have demonstrated how an understanding of natural and evolutionary history can
651 help to disentangle the putative agents of selection on an adaptive trait. Wing trait
652 differences across sexes, clades and environments give insight into the selective forces
653 driving phenotypic divergence in *Heliconius*, beyond the effects of natural selection imposed
654 by Müllerian mimicry. Our study highlights the complexity of selection pressures affecting
655 seemingly simple traits and the need for a thorough understanding of life history differences
656 amongst species.

657 *References*

- 658 Allen, C. E., B. J. Zwaan, and P. M. Brakefield. 2011. Evolution of Sexual Dimorphism in the
659 Lepidoptera. *Annual Review of Entomology*, doi: 10.1146/annurev-ento-120709-
660 144828.
- 661 Altizer, S., and A. K. Davis. 2010. Populations of monarch butterflies with different migratory
662 behaviors show divergence in wing morphology. *Evolution*, doi: 10.1111/j.1558-
663 5646.2009.00946.x.
- 664 Azevedo, R. B. R., A. C. James, J. McCabe, and L. Partridge. 2006. Latitudinal Variation of
665 Wing: Thorax Size Ratio and Wing-Aspect Ratio in *Drosophila melanogaster*.
666 *Evolution*, doi: 10.2307/2411305.
- 667 Bartón, K. 2018. MuMIn: Multi-Model Inference.
- 668 Beltrán, M., C. Jiggins, A. Brower, E. Bermingham, and J. Mallet. 2007. Do pollen feeding
669 and pupal-mating have a single origin in *Heliconius* butterflies? Inferences from
670 multilocus sequence data. *Biological Journal of the Linnean Society*.
- 671 Berwaerts, K., H. Van Dyck, and P. Aerts. 2002. Does flight morphology relate to flight
672 performance? An experimental test with the butterfly *Pararge aegeria*. *Functional*
673 *Ecology*, doi: 10.1046/j.1365-2435.2002.00650.x.
- 674 Betts, C. R., and R. J. Wootton. 1988. Wing shape and flight behaviour in butterflies
675 (Lepidoptera: Papilionoidea and Hesperioidea): a preliminary analysis. *Journal of*
676 *Experimental Biology*.
- 677 Bitner-Mathé, B. C., and L. B. Klaczko. 1999. Size and shape heritability in natural
678 populations of *Drosophila mediopunctata*: temporal and microgeographical variation.
679 *Heredity* 35–42.
- 680 Boggs, C. L. 1981. Selection Pressures Affecting Male Nutrient Investment at Mating in
681 Heliconiine Butterflies. *Evolution*, doi: 10.2307/2407864.
- 682 Breuker, C. J., P. M. Brakefield, and M. Gibbs. 2007. The association between wing
683 morphology and dispersal is sex-specific in the glanville fritillary butterfly *Melitae*

684 cinxia (Lepidoptera: Nymphalidae). *European Journal of Entomology*, doi:
685 10.14411/eje.2007.064.

686 Buler, J. J., R. J. Lyon, J. A. Smolinsky, T. J. Zenzal, and F. R. Moore. 2017. Body mass and
687 wing shape explain variability in broad-scale bird species distributions of migratory
688 passerines along an ecological barrier during stopover. *Oecologia*, doi:
689 10.1007/s00442-017-3936-y.

690 Cardoso, M. Z., J. J. Roper, and L. E. Gilbert. 2009. Prenuptial agreements: Mating
691 frequency predicts gift-giving in *Heliconius* species. *Entomologia Experimentalis et*
692 *Applicata*, doi: 10.1111/j.1570-7458.2009.00837.x.

693 Cardoso, M. Z., and E. S. Silva. 2015. Spermatophore Quality and Production in two
694 *Heliconius* Butterflies with Contrasting Mating Systems. *Journal of Insect Behavior*,
695 doi: 10.1007/s10905-015-9536-y.

696 Carreira, V. P., I. M. Soto, J. Mensch, and J. J. Fanara. 2011. Genetic basis of wing
697 morphogenesis in *Drosophila*: Sexual dimorphism and non-allometric effects of
698 shape variation. *BMC Developmental Biology*, doi: 10.1186/1471-213X-11-32.

699 Cespedes, A., C. M. Penz, and P. J. Devries. 2015. Cruising the rain forest floor: Butterfly
700 wing shape evolution and gliding in ground effect. *Journal of Animal Ecology*, doi:
701 10.1111/1365-2656.12325.

702 Chai, P., and R. B. Srygley. 1990. Predation and the Flight, Morphology, and Temperature of
703 Neotropical Rain-Forest Butterflies. *The American Naturalist* 135:748–765.

704 Chazot, N., S. Panara, N. Zilbermann, P. Blandin, Y. Le Poul, R. Cornette, M. Elias, and V.
705 Debat. 2016. *Morpho* morphometrics: Shared ancestry and selection drive the
706 evolution of wing size and shape in *Morpho* butterflies.

707 Chown, S. L., and K. J. Gaston. 2010. Body size variation in insects: A macroecological
708 perspective. *Biological Reviews* 85:139–169.

709 Classen, A., I. Steffan-Dewenter, W. J. Kindeketa, and M. K. Peters. 2017. Integrating
710 intraspecific variation in community ecology unifies theories on body size shifts along
711 climatic gradients. *Functional Ecology* 31:768–777.

712 Cook, L. M., E. W. Thomason, and A. M. Young. 1976. Population Structure, Dynamics and
713 Dispersal of the Tropical Butterfly *Heliconius charitonius*. *Journal of Animal Ecology*
714 45:851–863.

715 Deinert, E. I., J. T. Longino, and L. E. Gilbert. 1994. Mate competition in butterflies [5].
716 *Nature*, doi: 10.1038/370023a0.

717 Dell’Aglio, D. D., M. E. Losada, and C. D. Jiggins. 2016. Butterfly Learning and the
718 Diversification of Plant Leaf Shape. *Frontiers in Ecology and Evolution*, doi:
719 10.3389/fevo.2016.00081.

720 DeVries, P. J., C. M. Penz, and R. I. Hill. 2010. Vertical distribution, flight behaviour and
721 evolution of wing morphology in *Morpho* butterflies. *Journal of Animal Ecology*, doi:
722 10.1111/j.1365-2656.2010.01710.x.

723 Dillon, M. E. 2006. Into thin air: Physiology and evolution of alpine insects. *Integrative and*
724 *Comparative Biology* 46:49–61.

725 Dillon, M. E., M. R. Frazier, R. Dudley, S. Integrative, C. Biology, N. Feb, M. E. Dillon, M. R.
726 Frazier, and R. Dudleyt. 2018. Into Thin Air : Physiology and Evolution of Alpine
727 Insects Stable URL : <http://www.jstor.org/stable/3884976> REFERENCES Linked
728 references are available on JSTOR for this article : Into thin air : Physiology and
729 evolution of alpine insects. 46:49–61.

730 Dudley, R. 2002. The Biomechanics of Insect Flight: Form, Function, Evolution. *Annals of*
731 *the Entomological Society of America*, doi: 10.1093/aesa/93.5.1195f.

732 Dunn, P. O., J. K. Armenta, and L. A. Whittingham. 2015. Natural and sexual selection act
733 on different axes of variation in avian plumage color. *Science Advances*, doi:
734 10.1126/sciadv.1400155.

735 Farney, J., and E. D. Fleharty. 1969. Aspect Ratio, Loading, Wing Span, and Membrane
736 Areas of Bats. *Journal of Mammalogy*, doi: 10.2307/1378361.

737 Freckleton, R. P., P. H. Harvey, and M. Pagel. 2002. Phylogenetic Analysis and
738 Comparative Data: A Test and Review of Evidence. *The American Naturalist*, doi:
739 10.1086/343873.

740 Garamszegi, L. Z. 2014. Modern phylogenetic comparative methods and their application in
741 evolutionary biology.

742 García-Robledo, C., E. K. Kuprewicz, C. L. Staines, T. L. Erwin, and W. J. Kress. 2016.
743 Limited tolerance by insects to high temperatures across tropical elevational
744 gradients and the implications of global warming for extinction. *Proceedings of the*
745 *National Academy of Sciences* 113:680–685.

746 Gilchrist, A. S., R. B. R. Azevedo, L. Partridge, and P. O'Higgins. 2000. Adaptation and
747 constraint in the evolution of *Drosophila melanogaster* wing shape. *Evolution and*
748 *Development* 2:114–124.

749 Gilchrist, A. S., and L. Partridge. 2001. The contrasting genetic architecture of wing size and
750 shape in *Drosophila melanogaster*. *Heredity*, doi: 10.1046/j.1365-2540.2001.00779.x.

751 Ginestet, C. 2011. ggplot2: Elegant Graphics for Data Analysis. *Journal of the Royal*
752 *Statistical Society: Series A (Statistics in Society)*, doi: 10.1111/j.1467-
753 985X.2010.00676_9.x.

754 Grömping, U. 2006. Relative Importance for Linear Regression in *R*: The Package
755 **relaimpo**. *Journal of Statistical Software*, doi: 10.18637/jss.v017.i01.

756 Hurvich, C. M., and C.-L. Tsai. 1989. Regression and time series model selection in small
757 samples. *Biometrika* 76:297–307.

758 Jiggins, C. D. 2016. *The Ecology and Evolution of Heliconius Butterflies*. Oxford University
759 Press.

760 Jombart, T., and S. Dray. 2010. Adephylo: Exploratory Analyses for the Phylogenetic
761 Comparative Method. *Bioinformatics*, doi: 10.1093/bioinformatics/btq292.

762 Jones, R. T., Y. L. Poul, A. C. Whibley, C. Mérot, R. H. French-Constant, and M. Joron.
763 2013. Wing Shape Variation Associated With Mimicry In Butterflies. *Evolution*
764 67:2323–2334.

765 Joron, M. 2005. Polymorphic mimicry, microhabitat use, and sex-specific behaviour. *Journal*
766 *of Evolutionary Biology*, doi: 10.1111/j.1420-9101.2005.00880.x.

767 Karlsson, B. 1998. Nuptial gifts, resource budgets, and reproductive output in a polyandrous
768 butterfly. *Ecology*, doi: 10.1890/0012-9658(1998)079[2931:NGRBAR]2.0.CO;2.

769 Keck, F., F. Rimet, A. Bouchez, and A. Franc. 2016. Phylosignal: An R package to measure,
770 test, and explore the phylogenetic signal. *Ecology and Evolution*, doi:
771 10.1002/ece3.2051.

772 Kemp, D. J. 2019. Manipulation of natal host modifies adult reproductive behaviour in the
773 butterfly *Heliconius charithonia*. *Proceedings of the Royal Society B: Biological*
774 *Sciences* 286:20191225.

775 Klaczko, L. B. 1999. Size and shape heritability in natural populations of. *Heredity* 35–42.

776 Klepsatel, P., M. Gálíková, C. D. Huber, and T. Flatt. 2014. Similarities and differences in
777 altitudinal versus latitudinal variation for morphological traits in *Drosophila*
778 *melanogaster*. *Evolution* 68:1385–1398.

779 Kozak, K. M., W. O. McMillan, M. Joron, and C. D. Jiggins. 2018. Genome-wide admixture is
780 common across the *Heliconius* radiation. *Evolutionary Biology*.

781 Kozak, K. M., N. Wahlberg, A. F. E. Neild, K. K. Dasmahapatra, J. Mallet, and C. D. Jiggins.
782 2015. Multilocus species trees show the recent adaptive radiation of the mimetic
783 *Heliconius* butterflies. *Systematic Biology* 64:505–524.

784 Le Roy, C., V. Debat, and V. Llaurens. 2019. Adaptive evolution of butterfly wing shape:
785 from morphology to behaviour. *Biological Reviews*, doi: 10.1111/brv.12500.

786 Losos, J. B. 2010. Adaptive Radiation, Ecological Opportunity, and Evolutionary
787 Determinism. *The American Naturalist*, doi: 10.1086/652433.

788 Maia, R., D. R. Rubenstein, and M. D. Shawkey. 2016. Selection, constraint, and the
789 evolution of coloration in African starlings. *Evolution*, doi: 10.1111/evo.12912.

790 Marques, D. A., J. I. Meier, and O. Seehausen. 2019. A Combinatorial View on Speciation
791 and Adaptive Radiation.

792 Mendoza-Cuenca, L., and R. Macías-Ordóñez. 2010. Female asynchrony may drive
793 disruptive sexual selection on male mating phenotypes in a *Heliconius* butterfly.
794 *Behavioral Ecology* 21:144–152.

795 Mérot, C., Y. Le Poul, M. Théry, and M. Joron. 2016. Refining mimicry: phenotypic variation
796 tracks the local optimum. *The Journal of animal ecology*, doi: 10.1111/1365-
797 2656.12521.

798 Mérot, C., J. Mavárez, A. Evin, K. K. Dasmahapatra, J. Mallet, G. Lamas, and M. Joron.
799 2013. Genetic differentiation without mimicry shift in a pair of hybridizing *Heliconius*
800 species (Lepidoptera: Nymphalidae). *Biological Journal of the Linnean Society*
801 109:830–847.

802 Merrill, R. M., K. K. Dasmahapatra, J. W. Davey, D. D. Dell’Aglio, J. J. Hanly, B. Huber, C.
803 D. Jiggins, M. Joron, K. M. Kozak, V. Llaurens, S. H. Martin, S. H. Montgomery, J.
804 Morris, N. J. Nadeau, A. L. Pinharanda, N. Rosser, M. J. Thompson, S. Vanjari, R.
805 W. R. Wallbank, and Q. Yu. 2015. The diversification of *Heliconius* butterflies: What
806 have we learned in 150 years? *Journal of Evolutionary Biology* 28:1417–1438.

807 Merrill, R. M., R. W. R. Wallbank, V. Bull, P. C. A. Salazar, J. Mallet, M. Stevens, and C. D.
808 Jiggins. 2012. Disruptive ecological selection on a mating cue. *Proceedings of the*
809 *Royal Society B: Biological Sciences*, doi: 10.1098/rspb.2012.1968.

810 Münkemüller, T., S. Lavergne, B. Bzeznik, S. Dray, T. Jombart, K. Schiffers, and W. Thuiller.
811 2012. How to measure and test phylogenetic signal. *Methods in Ecology and*
812 *Evolution* 3:743–756.

813 Nadeau, N. J., C. Pardo-Diaz, A. Whibley, M. A. Supple, S. V. Saenko, R. W. R. Wallbank,
814 G. C. Wu, L. Maroja, L. Ferguson, J. J. Hanly, H. Hines, C. Salazar, R. M. Merrill, A.
815 J. Dowling, R. H. Ffrench-Constant, V. Llaurens, M. Joron, W. O. McMillan, and C. D.
816 Jiggins. 2016. The gene cortex controls mimicry and crypsis in butterflies and moths.
817 *Nature*, doi: 10.1038/nature17961.

818 Nakagawa, S., and H. Schielzeth. 2013. A general and simple method for obtaining R² from
819 generalized linear mixed-effects models. *Methods in Ecology and Evolution* 4:133–
820 142.

821 Nosil, P., R. Villoutreix, C. F. De Carvalho, T. E. Farkas, V. Soria-Carrasco, J. L. Feder, B. J.
822 Crespi, and Z. Gompert. 2018. Natural selection and the predictability of evolution in
823 timema stick insects. *Science*, doi: 10.1126/science.aap9125.

824 Ortega Ancel, A., R. Eastwood, D. Vogt, C. Ithier, M. Smith, R. Wood, and M. Kovač. 2017.
825 Aerodynamic evaluation of wing shape and wing orientation in four butterfly species
826 using numerical simulations and a low-speed wind tunnel, and its implications for the
827 design of flying micro-robots. *Interface Focus* 7:20160087.

828 Outomuro, D., and F. Johansson. 2017. A potential pitfall in studies of biological shape:
829 Does size matter? *Journal of Animal Ecology*, doi: 10.1111/1365-2656.12732.

830 Paradis, E. 2012. *Analysis of phylogenetics and evolution with R: Second edition*.

831 Pinheiro, J., D. Bates, S. DebRoy, and D. Sarkar. 2007. *nlme: Linear and Nonlinear Mixed*
832 *Effects Models*. R Development Core Team, doi: Doi 10.1038/Ncb1288.

833 Pitchers, W., J. E. Pool, and I. Dworkin. 2012. ALTITUDINAL CLINAL VARIATION IN WING
834 SIZE AND SHAPE IN AFRICAN DROSOPHILA MELANOGASTER : ONE CLINE OR
835 MANY ? , doi: 10.5061/dryad.r43k1.

836 Pyrcz, T. W., K. Sattler, D. C. Lees, G. W. Beccaloni, J. R. Ferrer-Paris, J. Wojtusiak, and A.
837 L. Vilorio. 2004. A brachypterous butterfly? *Proceedings of the Royal Society of*
838 *London. Series B: Biological Sciences*, doi: 10.1098/rsbl.2003.0015.

839 Queiroz, A. de, and K. G. Ashton. 2004. The phylogeny of a species-level tendency: species
840 heritability and possible deep origins of Bergmann's rule in tetrapods. *evol* 58:1674–
841 1684.

842 Ray, R. P., T. Nakata, P. Henningsson, and R. J. Bomphrey. 2016. Enhanced flight
843 performance by genetic manipulation of wing shape in *Drosophila*. *Nat Commun* 7:1–
844 8.

845 Revell, L. J. 2010. Phylogenetic signal and linear regression on species data. *Methods in*
846 *Ecology and Evolution*, doi: 10.1111/j.2041-210X.2010.00044.x.

847 Rodrigues, D., and G. R. P. Moreira. 2002. Geographical variation in larval host-plant use by
848 *Heliconius erato* (Lepidoptera: Nymphalidae) and consequences for adult life history.
849 *Brazilian Journal of Biology* 62:321–32.

850 Rodrigues, D., and G. R. P. Moreira. 2004. Seasonal variation in larval host plants and
851 consequences for *Heliconius erato* (Lepidoptera: Nymphalidae) adult body size.
852 *Austral Ecology* 29:437–445.

853 Rossato, D. O., D. Boligon, R. Fornel, M. R. Kronforst, G. L. Gonçalves, and G. R. P.
854 Moreira. 2018a. Subtle variation in size and shape of the whole forewing and the red
855 band among co-mimics revealed by geometric morphometric analysis in *Heliconius*
856 butterflies. *Ecology and Evolution*, doi: 10.1002/ece3.3916.

857 Rossato, D. O., L. A. Kaminski, C. A. Iserhard, and L. Duarte. 2018b. More Than Colours:
858 An Eco-Evolutionary Framework for Wing Shape Diversity in Butterflies. P. *in*
859 *Advances in Insect Physiology*.

860 Rosser, N., A. V. L. Freitas, B. Huertas, M. Joron, G. Lamas, C. Mérot, F. Simpson, K. R.
861 Willmott, J. Mallet, and K. K. Dasmahapatra. 2019. Cryptic speciation associated with
862 geographic and ecological divergence in two Amazonian *Heliconius* butterflies. *Zool*
863 *J Linn Soc* 186:233–249.

864 Rosser, N., K. M. Kozak, A. B. Phillimore, and J. Mallet. 2015. Extensive range overlap
865 between heliconiine sister species: evidence for sympatric speciation in butterflies?
866 *BMC Evolutionary Biology* 15:125. *BMC Evolutionary Biology*.

867 Satterfield, D. A., and A. K. Davis. 2014. Variation in wing characteristics of monarch
868 butterflies during migration: Earlier migrants have redder and more elongated wings.
869 *Animal Migration*, doi: 10.2478/ami-2014-0001.

870 Schluter, D. 2000. *The Ecology of Adaptive Radiation*. Oxford Series in Ecology and
871 *Evolution*, doi: 10.2307/3558417.

872 Schulz, S., C. Estrada, S. Yildizhan, M. Boppré, and L. E. Gilbert. 2008. An antiaphrodisiac
873 in *Heliconius melpomene* butterflies. *Journal of Chemical Ecology*, doi:
874 10.1007/s10886-007-9393-z.

875 Shelomi, M. 2012. Where Are We Now? Bergmann's Rule Sensu Lato in Insects. The
876 American Naturalist 180:511–519.

877 Singer, M. C. 1982. Sexual Selection for Small Size in Male Butterflies. The American
878 Naturalist, doi: 10.1086/283924.

879 Srygley, R. B. 1994. Locomotor Mimicry in Butterflies? The Associations of Positions of
880 Centres of Mass among Groups of Mimetic, Unprofitable Prey. Philosophical
881 Transactions of the Royal Society B: Biological Sciences, doi:
882 10.1098/rstb.1994.0017.

883 Srygley, R. B. 2004a. The aerodynamic costs of warning signals in palatable mimetic
884 butterflies and their distasteful models. Proceedings of the Royal Society B:
885 Biological Sciences, doi: 10.1098/rspb.2003.2627.

886 Srygley, R. B. 2004b. The aerodynamic costs of warning signals in palatable mimetic
887 butterflies and their distasteful models. Proceedings of the Royal Society B:
888 Biological Sciences, doi: 10.1098/rspb.2003.2627.

889 Stalker, H. D., and H. L. Carson. 1948. An Altitudinal Transect of *Drosophila robusta*
890 Sturtevant. *Evolution* 2:295–305.

891 Stillwell, R. C., W. U. Blanckenhorn, T. Teder, G. Davidowitz, and C. W. Fox. 2010. Sex
892 Differences in Phenotypic Plasticity Affect Variation in Sexual Size Dimorphism in
893 Insects: From Physiology to Evolution. *Annual Review of Entomology*, doi:
894 10.1146/annurev-ento-112408-085500.

895 Stoffel, M. A., S. Nakagawa, and H. Schielzeth. 2017. rptR: repeatability estimation and
896 variance decomposition by generalized linear mixed-effects models.

897 Thurman, T. J., E. Brodie, E. Evans, and W. O. McMillan. 2018. Facultative pupal mating in
898 *Heliconius erato*: Implications for mate choice, female preference, and speciation.
899 *Ecology and Evolution* 8:1882–1889.

900 Wootton, R. 2002. Functional Morphology Of Insect Wings. *Annual Review of Entomology*,
901 doi: 10.1146/annurev.ento.37.1.113.

903
904
905
906
907
908

Supplementary Materials

Table S1 Study species summary data. Sample sizes (N) and wing parameters for the 13 study species, ordered phylogenetically based on the most recent *Heliconius* phylogeny (Kozak et al. 2015). Male ratio refers to proportion of males in the sample.

Species	N	Area mean (mm ²)	Area S.E.	Aspect ratio mean	Aspect ratio S.E.	Alt. mean (m.a.s.l.)	N _{male}	N _{female}	Male ratio
<i>H. telesiphe</i>	48	519.4	8.9	2.35	0.009	1302	40	8	0.83
<i>H. clysonymus</i>	57	537.3	8.4	2.31	0.012	1346	40	17	0.70
<i>H. erato</i>	1687	465.8	1.5	2.09	0.002	700	1202	447	0.73
<i>H. eleuchia</i>	102	500.6	8.6	2.03	0.007	1408	72	30	0.71
<i>H. sara</i>	225	387.2	2.9	2.17	0.006	420	164	61	0.73
<i>H. xanthocles</i>	36	514.6	10.3	2.04	0.009	1044	20	8	0.71
<i>H. hierax</i>	37	512.1	8.3	2.08	0.008	1364	29	8	0.78
<i>H. doris</i>	42	547.5	7.1	2.30	0.012	444	34	7	0.83
<i>H. timareta</i>	195	606.7	3.1	2.05	0.004	883	163	32	0.84
<i>H. cydno</i>	127	575.1	5.5	2.09	0.007	844	112	15	0.88
<i>H. melpomene</i>	867	533.3	1.9	2.05	0.002	789	683	159	0.81
<i>H. numata</i>	44	611.6	12.9	2.11	0.013	561	30	14	0.68
<i>H. wallacei</i>	48	526.3	8.2	2.18	0.011	290	37	11	0.77

909
910

911
 912
 913
 914
 915

Table S2. Study species sexual dimorphism. Sexual size dimorphism (SSD) and sexual shape dimorphism (SShD) two-sample t-tests summary statistics. Positive t-values indicate smaller or longer-winged (higher aspect ratio) males (Fig. 2, main text).

Species	SSD t-value	SSD d.f.	SSD p-value	SShD t-value	SShD d.f.	SShD p-value
<i>H. telesiphe</i>	2.57	10	<0.05*	-0.5	10	ns
<i>H. clysonymus</i>	1.98	24	0.06•	-1.5	39	ns
<i>H. erato</i>	3.30	802	<0.001***	10.4	843	<0.001***
<i>H. eleuchia</i>	-2.61	61	<0.01**	-2.3	48	<0.05*
<i>H. sara</i>	-2.45	108	<0.05*	-0.6	100	ns
<i>H. xanthocles</i>	-0.08	13	ns	0.5	13	ns
<i>H. hierax</i>	-0.50	8	ns	0.5	16	ns
<i>H. doris</i>	-1.92	9	0.08•	1.4	11	ns
<i>H. timareta</i>	2.03	49	0.05•	-0.2	46	ns
<i>H. cydno</i>	0.57	18	ns	0.1	16	ns
<i>H. melpomene</i>	5.54	240	<0.001***	1.6	230	ns
<i>H. numata</i>	2.57	24	<0.05*	-0.9	33	ns
<i>H. wallacei</i>	-1.31	16	ns	2.2	19	<0.05*

916

917 **Table S3.** Weighted PGLS model selection table for species sexual size dimorphism
 918 (SSD), mean wing aspect ratio and mean wing area based on AICc. All models have
 919 the species phylogeny as correlation structure and are weighted for mean trait/fixed
 920 effects variance and sample size.

921

Size sexual dimorphism (SSD)

Minimal model $\text{sisd.raw} \sim 1$
 Maximal model $\text{sisd.raw} \sim \text{larva} + \text{shape.mean} + \text{shsd.raw} + \text{size.mean} + \text{clade}$
 Final model $\text{sisd.raw} \sim \text{larva} + \text{shsd.raw} + \text{shape.mean}$

Step	Df	Resid. Dev.	AICc
Initial model	6	73.7	109.8
-clade	7	73.46	99.5
-size.mean	8	75.6	93.7

922

Wing area (size)

Minimal model $\text{area.mean} \sim 1$
 Maximal model $\text{area.mean} \sim \text{shape.mean} * \text{sex.ratio} + \text{alt.mean} * \text{dist.Eq}$
 Final model $\text{area.mean} \sim \text{sex.ratio} + \text{alt.mean} + \text{dist.Eq} + \text{alt.mean} * \text{lat.mean}$

Step	Df	Resid. Dev.	AICc
Initial model	6	129.5	165.9
-shape.mean*sex.ratio	6	126.0	162.4
-shape.mean	7	126.0	152.0

923

924

Wing aspect ratio (shape)

Minimal model $\text{shape.mean} \sim 1$
 Maximal model $\text{shape.mean} \sim \text{size.mean} * \text{sex.ratio} + \text{alt.mean} * \text{dist.Eq}$
 Final model $\text{shape.mean} \sim \text{sex.ratio} + \text{alt.mean} + \text{dist.Eq}$

Step	Df	Resid. Dev.	AICc
Initial model	5	-20.4	31.6
alt.mean*lat.mean	6	-19.3	17.1
- alt.mean*size.mean	7	-17.8	8.2
- size.mean	8	-17.3	1.3

925

926

927
928
929
930
931

Table S4. Phylogenetic Generalised Least Squares full model summaries for sexual size dimorphism, wing shape and wing size. Correlation structures of the models are shown in the third column. Dist. Eq.= distance from Equator, SD= sexual dimorphism.

Response variable (wing trait)	Model type	Corr. structure	Fixed effects	Estimate	SE	t-value	p-value	d.f. (d.f. res.)
Size Sexual Dimorphism	PGLS (nmle)	Phylogeny, sample size	(Intercept)	-31.8	21.4	-1.5	0.08	13 (9)
			Solitary larvae	-15.8	3.0	-5.3	0.0004***	
			Shape sex dim.	1.8	1.3	1.5	0.2	
			Shape mean	17.8	10.3	1.8	0.1	
Aspect ratio	PGLS (nmle)	Phylogeny, intra-sp variance, sample size	(Intercept)	1.93	0.23	8.36	0.00	13 (9)
			Altitude	-1.5E-4	6.3E-5	-2.4	0.04*	
			Dist. Eq	-4.6E-2	1.7E-2	-2.7	0.02*	
			Sex ratio	0.70	0.28	2.5	0.03*	
Area	PGLS (nmle)	Phylogeny, intra-sp variance, sample size	(Intercept)	474.52	75.37	6.30	0.00	13 (8)
			Altitude	0.16	0.04	3.47	0.008**	
			Sex ratio	-161.75	73.97	-2.19	0.06	
			Dist. Eq.	77.21	16.91	4.57	0.002**	
			Altitude* Dist. Eq	-0.07	0.02	-4.66	0.002**	

932
933

934
935
936

Table S5. Model selection based on AIC of within species variation in wing aspect ratio and wing area of *H. erato* and *H. melpomene*.

A) Aspect ratio, *H. erato*

Minimal model aspect.ratio ~ 1
 Maximal model aspect.ratio ~ area.mm2 * altitude + dist.Eq. + longitude + sex
 Final model aspect.ratio ~ area.mm2 * altitude + longitude + sex

Step	Res. Df	Res. Dev.	AIC
Initial model	1294	4.92	-7246
- dist.Eq.	1295	4.92	-7248

937

B) Aspect ratio, *H. melpomene*

Minimal model aspect.ratio ~ 1
 Maximal model aspect.ratio ~ area.mm2 * altitude + dist.Eq. + longitude + sex
 Final model aspect.ratio ~ area.mm2 * altitude + longitude + sex

Step	Res. Df	Res. Dev.	AIC
Initial model	704	2.3	-4070
- dist.Eq.	705	2.3	-4072

938

C) Wing area, *H. erato*

Minimal model area ~ 1
 Maximal model area ~ aspect.ratio * altitude + dist.Eq + longitude + sex
 Final model area ~ aspect.ratio * altitude + dist.Eq + longitude + sex

Step	Res. Df	Res. Dev.	AIC
Initial model	1294	4841609	10720

939

D) Wing area, *H. melpomene*

Minimal model area ~ 1
 Maximal model area ~ aspect.ratio * altitude + dist.Eq + longitude + sex
 Final model area ~ aspect.ratio * altitude + dist.Eq + longitude + sex

Step	Res. Df	Res. Dev.	AIC
Initial model	704	2092210	5701

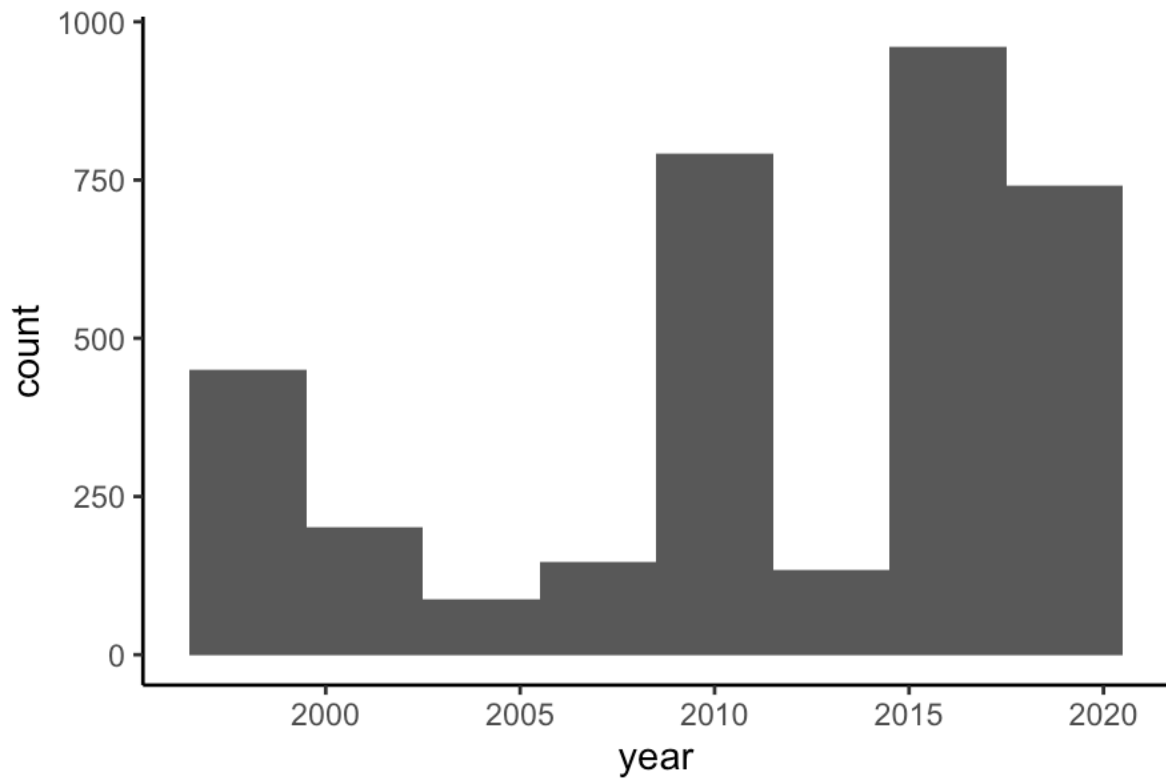
940

941
942
943
944
945

Table S6. Full model output table for within-species (*H. erato* and *H. melpomene*) analyses of wing aspect ratio and wing area. Relative R² per fixed effect estimated with the package *relaimpo* (Grömping 2006) and the *lmg* statistic.

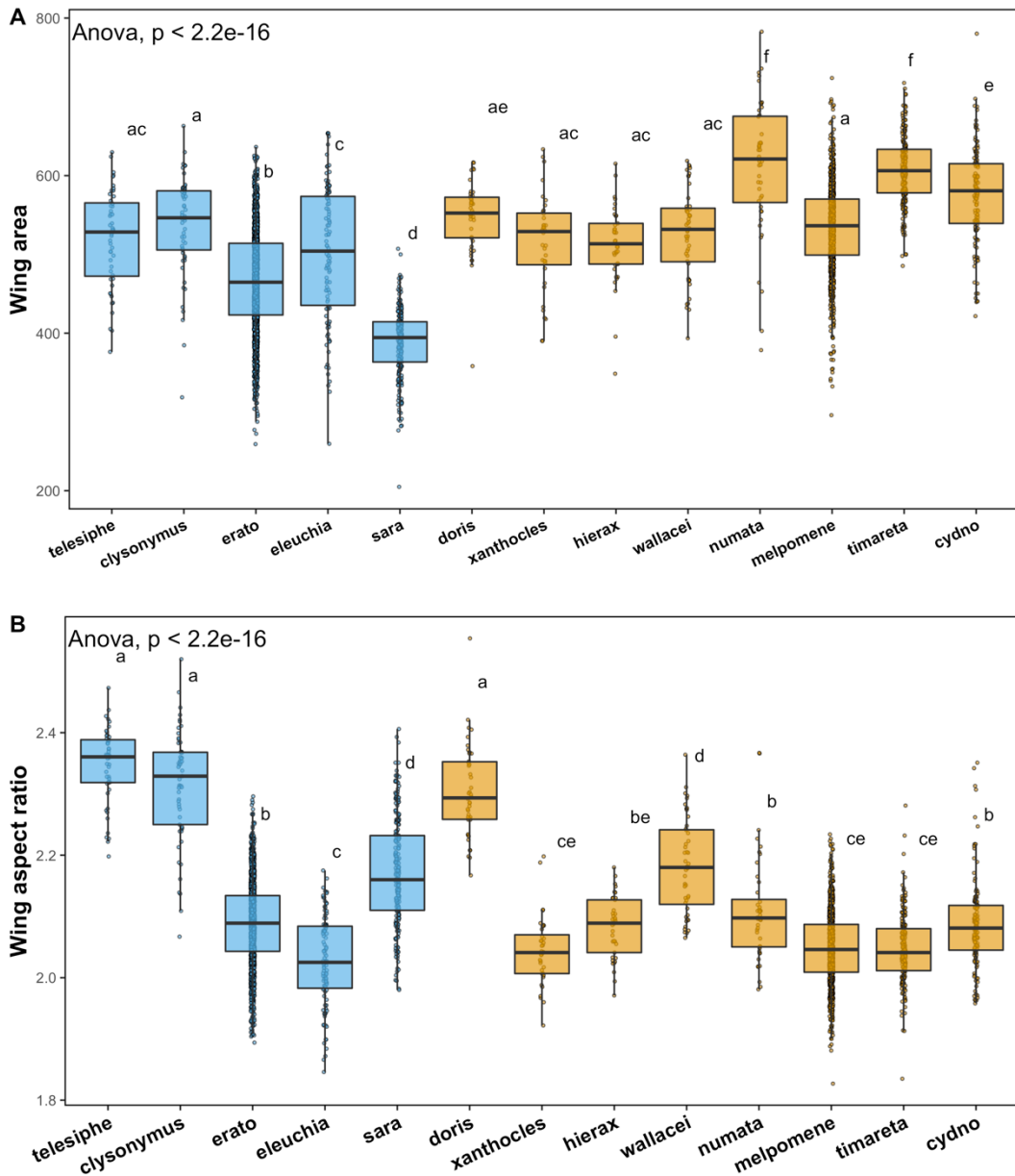
Trait (response)	Sp.	Fixed effects	Res. d.f.	Estimate	SE	t-value	p-value	Rel. R ²
Aspect ratio	<i>H. era.</i>	(intercept)	1295	2.2	0.03	75.57	0.00	
		altitude		-1.6E-04	0.00	-6.50	0.00***	0.43
		sex(female)		-3.4E-02	0.01	-2.87	0.004**	0.37
		area		-1.8E-04	0.00	-3.73	0.00***	0.14
		longitude		4.9E-04	0.00	2.00	0.05	0.05
		area*alt.		2.9E-07	0.00	5.30	0.00***	0.02
	<i>H. melp.</i>	(intercept)	705	2.3E+00	4.2E-02	55.08	0.00	
		altitude		-1.4E-04	3.4E-05	-4.17	0.00***	0.50
		area		-3.4E-04	6.1E-05	-5.63	0.00***	0.23
		area*alt.		2.2E-07	6.4E-08	3.40	0.001**	0.10
		longitude		6.6E-04	2.6E-04	2.53	0.012*	0.09
		sex(female)		-4.0E-02	1.3E-02	-3.16	0.001**	0.08
sex(male)	-3.1E-02	1.2E-02	-2.65	0.008**	(0.08)			
Wing area	<i>H. era.</i>	(intercept)	1294	879	102.27	8.60	0.00	
		AR*alt.		0.25	0.05	4.80	0.00***	0.38
		longitude		0.87	0.25	3.54	0.00***	0.18
		sex(female)		-19.3	11.90	-1.62	0.1	0.16
		sex(male)		-6.76	11.64	-0.58	0.56	0.15
		dist.Eq.		-2.35	0.84	-2.80	0.005**	(0.15)
		altitude		-0.53	0.11	-4.88	0.00***	0.08
		aspect.ratio		-161	47.56	-3.40	0.00***	0.05
	<i>H. melp.</i>	(intercept)	704	1430	131.35	10.89	0.00	
		dist.Eq.		-5.51	0.86	-6.38	0.00***	0.33
		longitude		1.51	0.24	6.21	0.00***	0.18
		sex(female)		-39.5	12.13	-3.26	0.001**	0.18
		sex(male)		-13.8	11.39	-1.21	0.23	(0.18)
		aspect.ratio		-365	61.86	-5.91	0.00***	0.15
AR*alt.	0.25	0.06	3.95	0.00***	0.10			
altitude	-0.51	0.13	-3.92	0.00***	0.05			

946
947



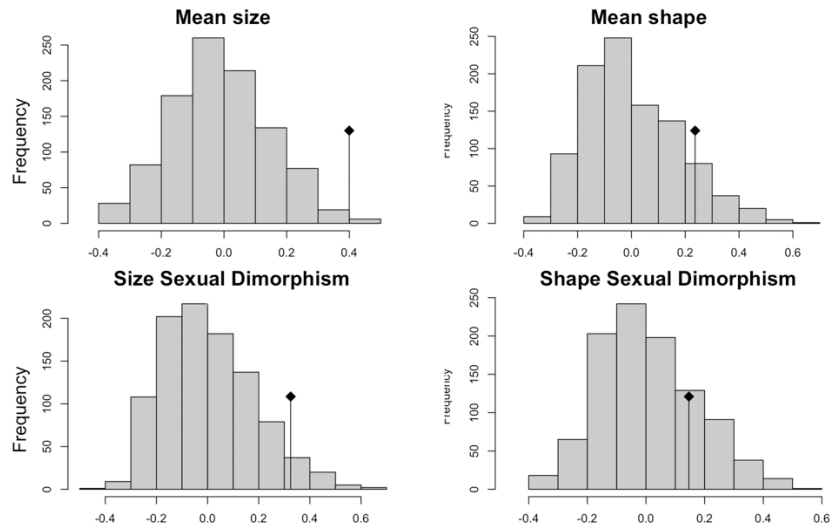
948
949
950
951
952

Figure S1. Number of *Heliconius* individuals in this study collected across 3-year intervals.



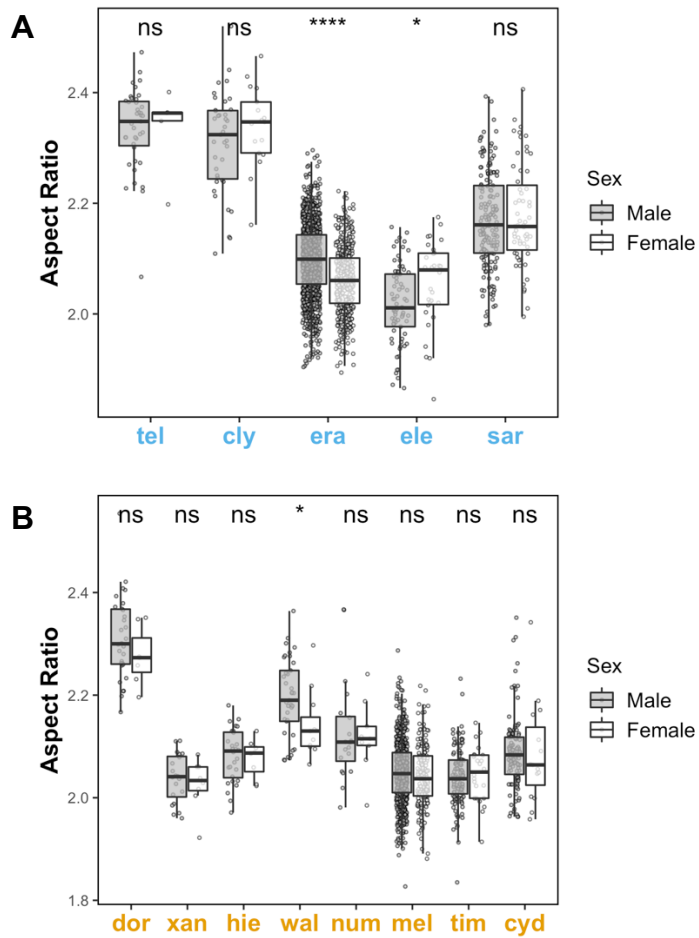
953
 954
 955
 956
 957
 958

Figure S2. Wing area (mm^2 , A) and wing aspect ratio (wing roundness, B) variation across species. Species sharing a letter are not significantly different (Tukey-adjusted comparisons). Species are ordered phylogenetically (for phylogeny see Fig. 3) and coloured by the two major clades.



959
 960
 961
 962
 963
 964
 965
 966
 967
 968

Figure S3. Abouheif C-mean distribution plots for six variables. Black dots depicts the observed C-mean statistic relative to the null hypothesis of randomisations along the tips of the phylogeny.



969
970

Figure S4. Sexual wing aspect ratio dimorphism across species of the erato clade

971

(A) and the melpomene clade (B). Wing aspect ratio differences between males

972

(grey) and females (white). Error bars represent 95% confidence intervals of the

973

means. Stars represent significance levels of two sample t-tests between female and

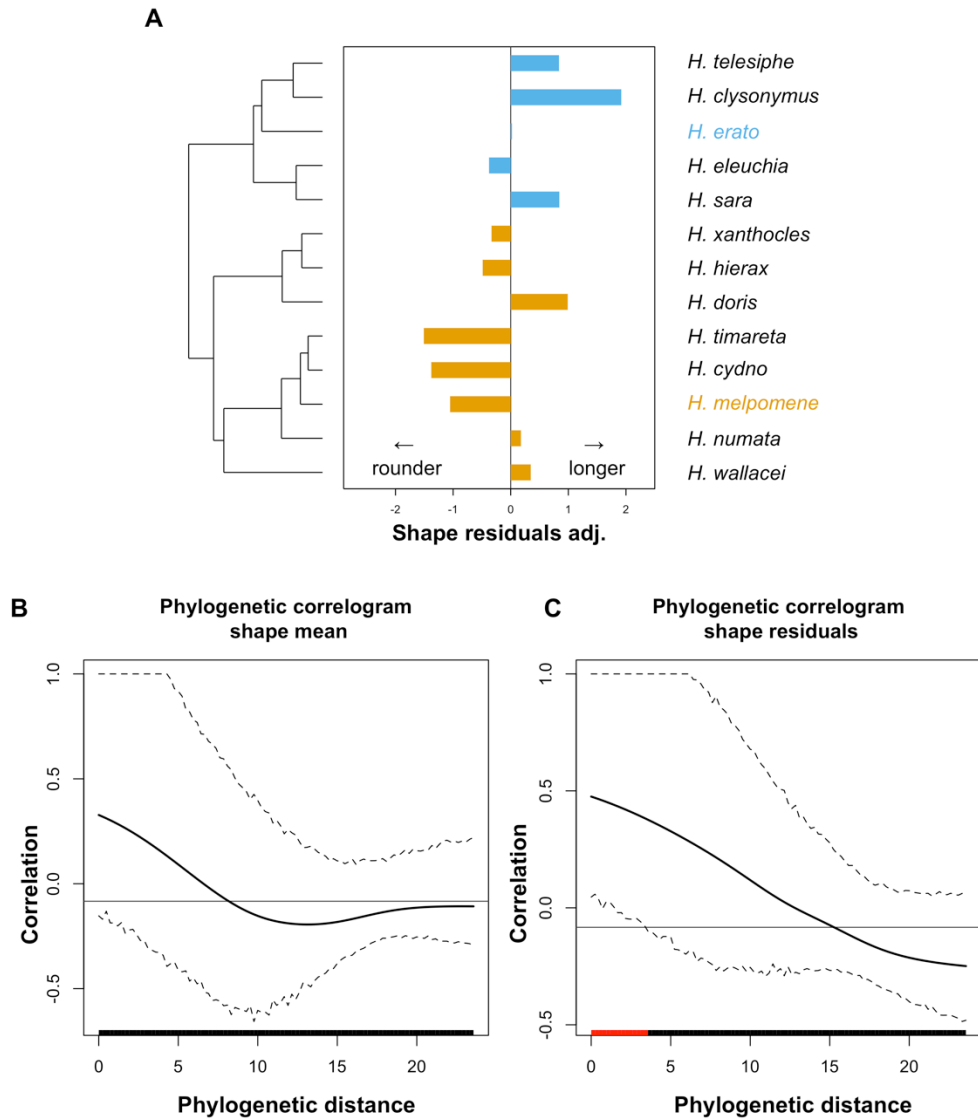
974

male wing areas for each species ($\bullet < 0.08$, $* < 0.05$, $** < 0.01$, $*** < 0.001$), for full t-tests

975

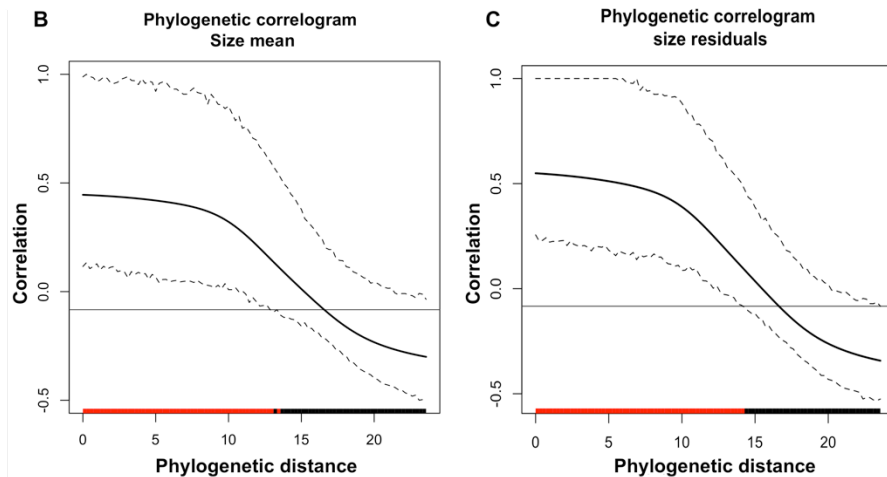
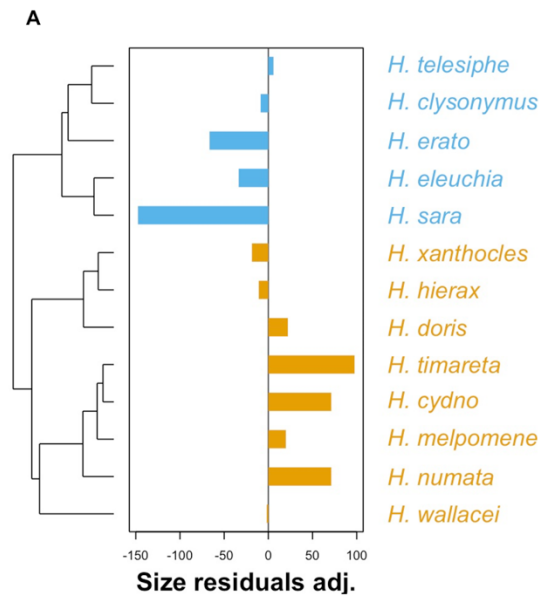
output see Table S2.

976



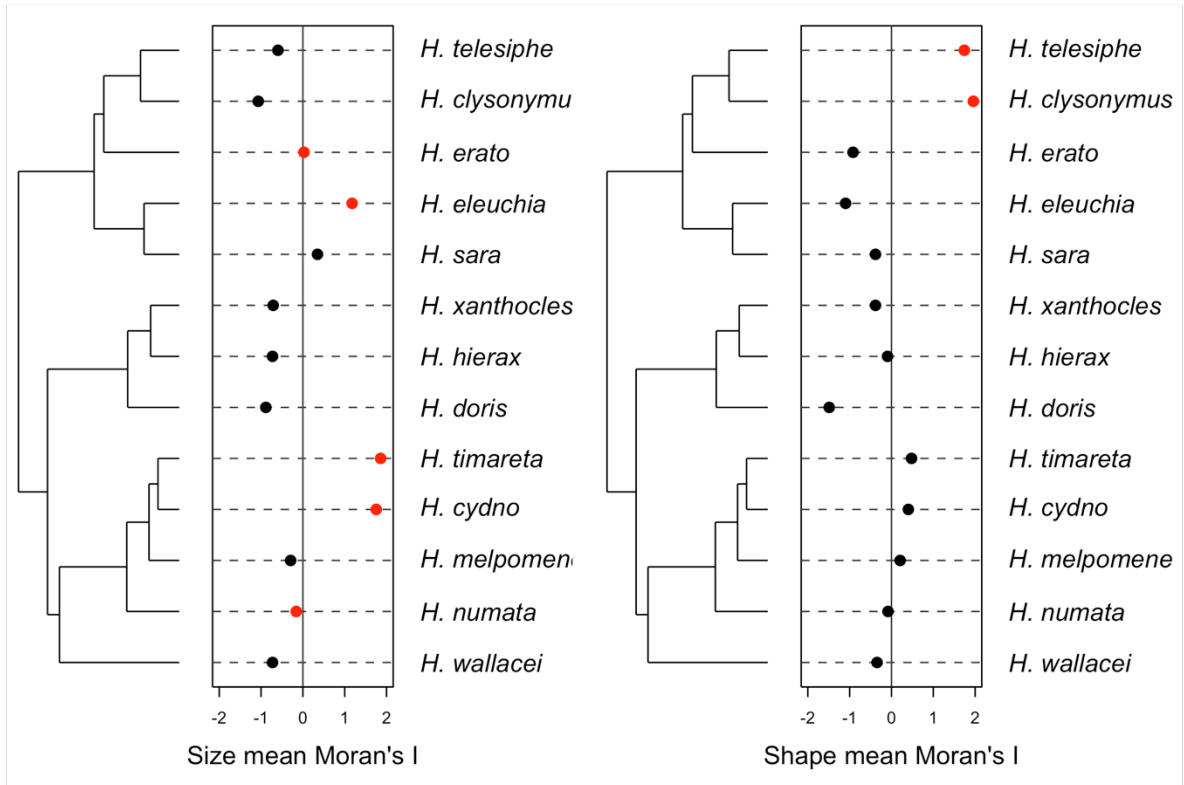
977
 978
 979
 980
 981
 982
 983
 984
 985
 986
 987
 988
 989
 990

Figure S5. Phylogenetic signal in wing shape. A) Z-transformed wing shape residuals across the *Heliconius* phylogeny. B) phylogenetic correlogram of species mean wing shape. C) phylogenetic correlogram of species wing shape model residuals. The solid black line represents Moran's I index of autocorrelation and the dashed black lines represent the lower and upper bounds of the confidence 95% confidence interval. The horizontal black line represents the expected value of Moran's I under the null hypothesis of no phylogenetic autocorrelation. The coloured bars in the x-axes show whether the autocorrelation is significant (based on the confidence interval): red for significant positive autocorrelation and black for nonsignificant autocorrelation. All figures were obtained with the package phylosignal (Keck et al. 2016).



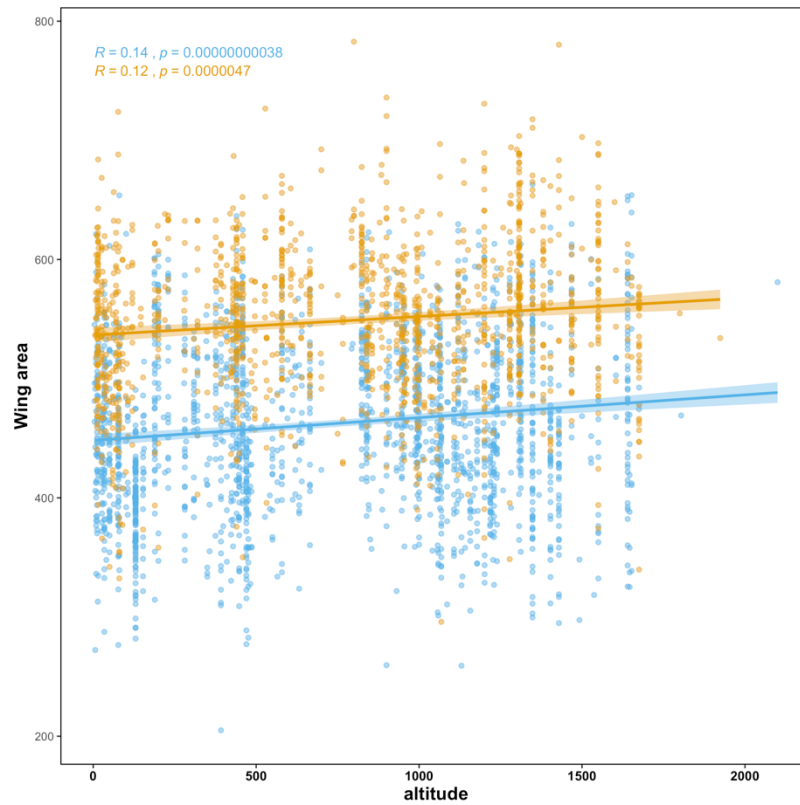
991
 992
 993
 994
 995
 996
 997
 998
 999
 1000
 1001
 1002
 1003

Figure S6. Phylogenetic signal in wing size. A) Centered wing size residuals across the *Heliconius* phylogeny. B) phylogenetic correlogram of species mean wing size. C) phylogenetic correlogram of species wing size model residuals. The solid black line represents Moran's I index of autocorrelation and the dashed black lines represent the lower and upper bounds of the confidence 95% confidence interval. The horizontal black line represents the expected value of Moran's I under the null hypothesis of no phylogenetic autocorrelation. The coloured bars in the x-axes show whether the autocorrelation is significant (based on the confidence interval): red for significant positive autocorrelation and black for nonsignificant autocorrelation.



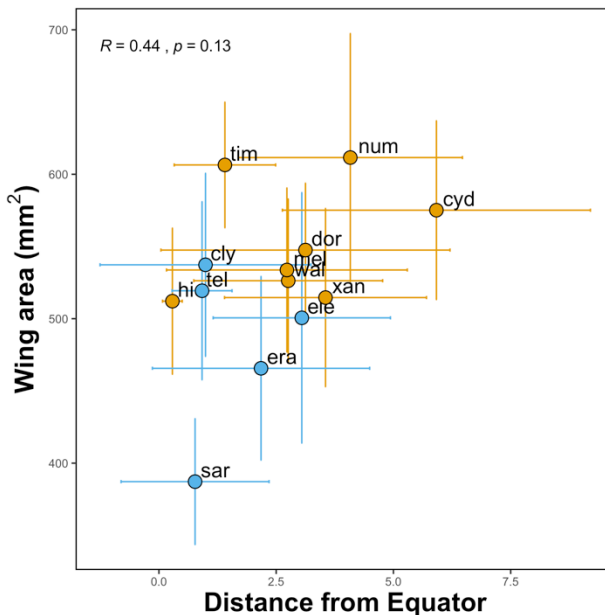
1004
 1005
 1006
 1007
 1008
 1009
 1010

Figure S7. Local Moran's I index values for each species for wing area mean (left) and wing aspect ratio mean (right). Red points indicate significant positive autocorrelation in mean traits among neighbours in the phylogeny. Estimated and plotted with the package *phylosignal* (Keck et al. 2016).



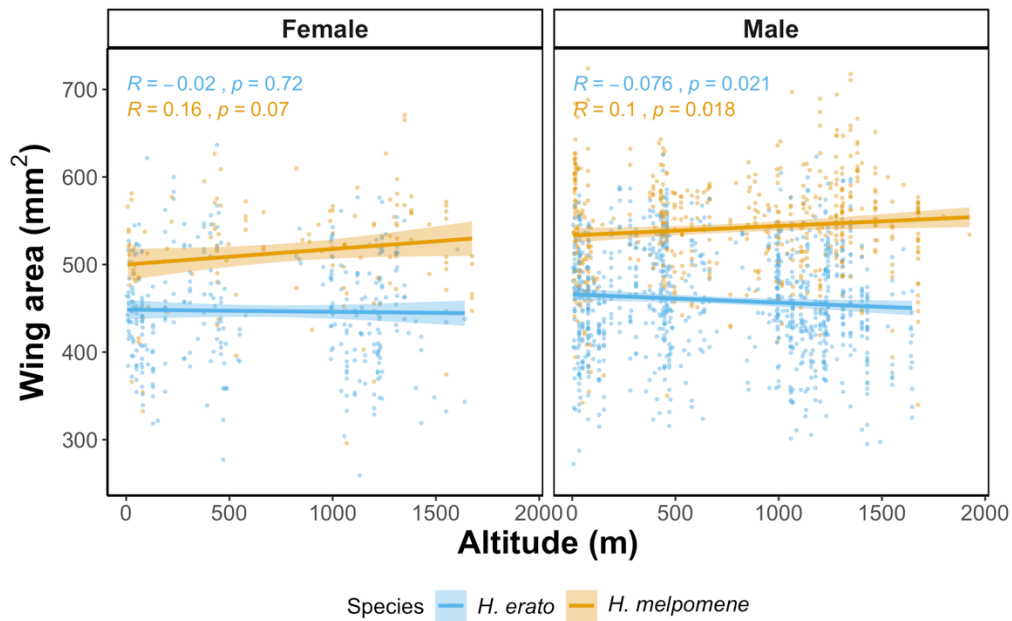
1011
1012
1013
1014
1015
1016
1017
1018

Figure S8. Wing area variation with altitude across individuals from all species of the erato clade (blue) and the melpomene clade (orange). Each point represents an individual. Lines show best linear fit and are colored by clade. Shaded areas show confidence bands at 1 standard error. Pearson correlation coefficients and p-values are shown for each regression plotted.



1020
 1021
 1022
 1023
 1024
 1025
 1026
 1027
 1028

Figure S9. Species variation in wing area. Plot shows the correlation between distance from the Equator (degrees) and species mean wing area (mm²). Points represent species mean raw values per species. Horizontal and vertical lines show standard error for species mean distance from Equator and mean wing area, respectively. The point labels correspond to the first three characters of the following *Heliconius* species: *H. telesiphe*, *H. clysonymus*, *H. erato*, *H. eleuchia*, *H. sara*, *H. doris*, *H. xanthocles*, *H. hierax*, *amH. wallacei*, *H. numata*, *H. melpomene*, *H. timareta*, *H. cydno*.



1030

1031

1032

1033

1034

1035

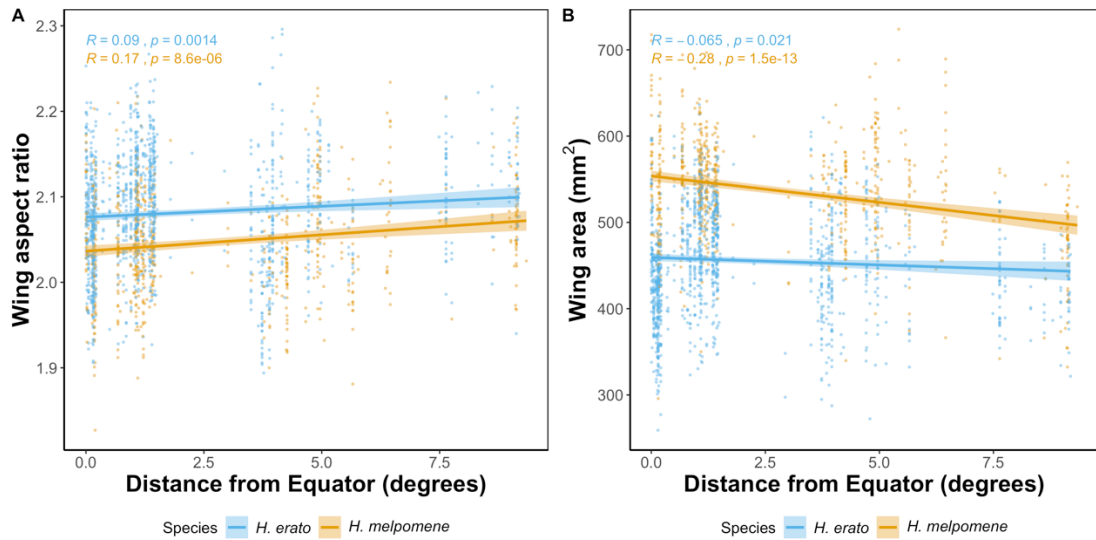
1036

1037

1038

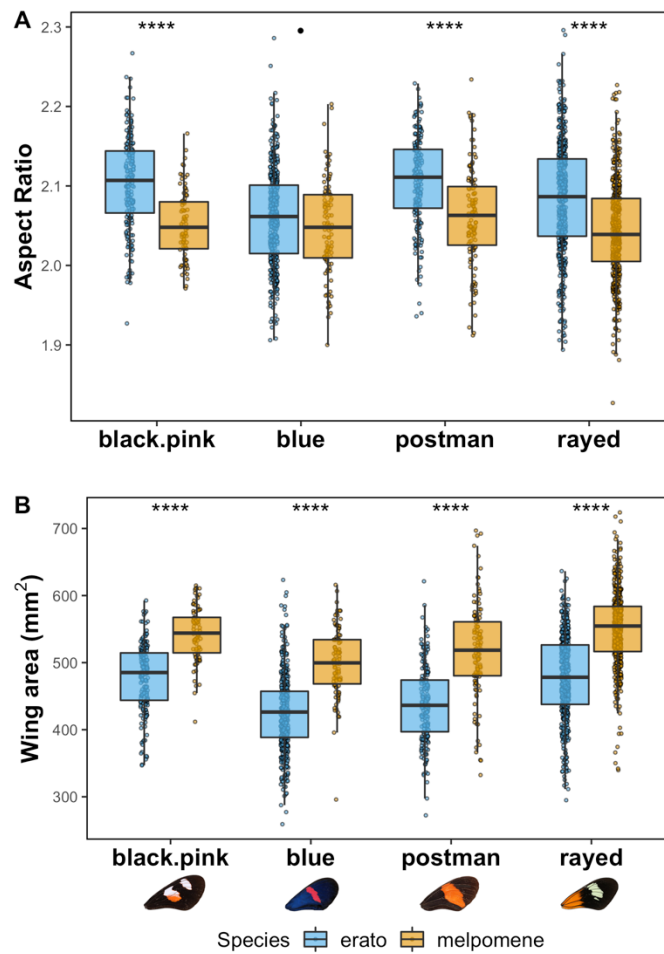
1039

Figure S10. Within-species variation in wing area (mm²) across alt.s in *H. erato* (blue) and *H. melpomene* (orange), females (left) and males (right). Lines show best linear fit and are colored by species. Shaded areas show confidence bands at 1 standard error. Pearson correlation coefficients and p-values are shown for each regression plotted.



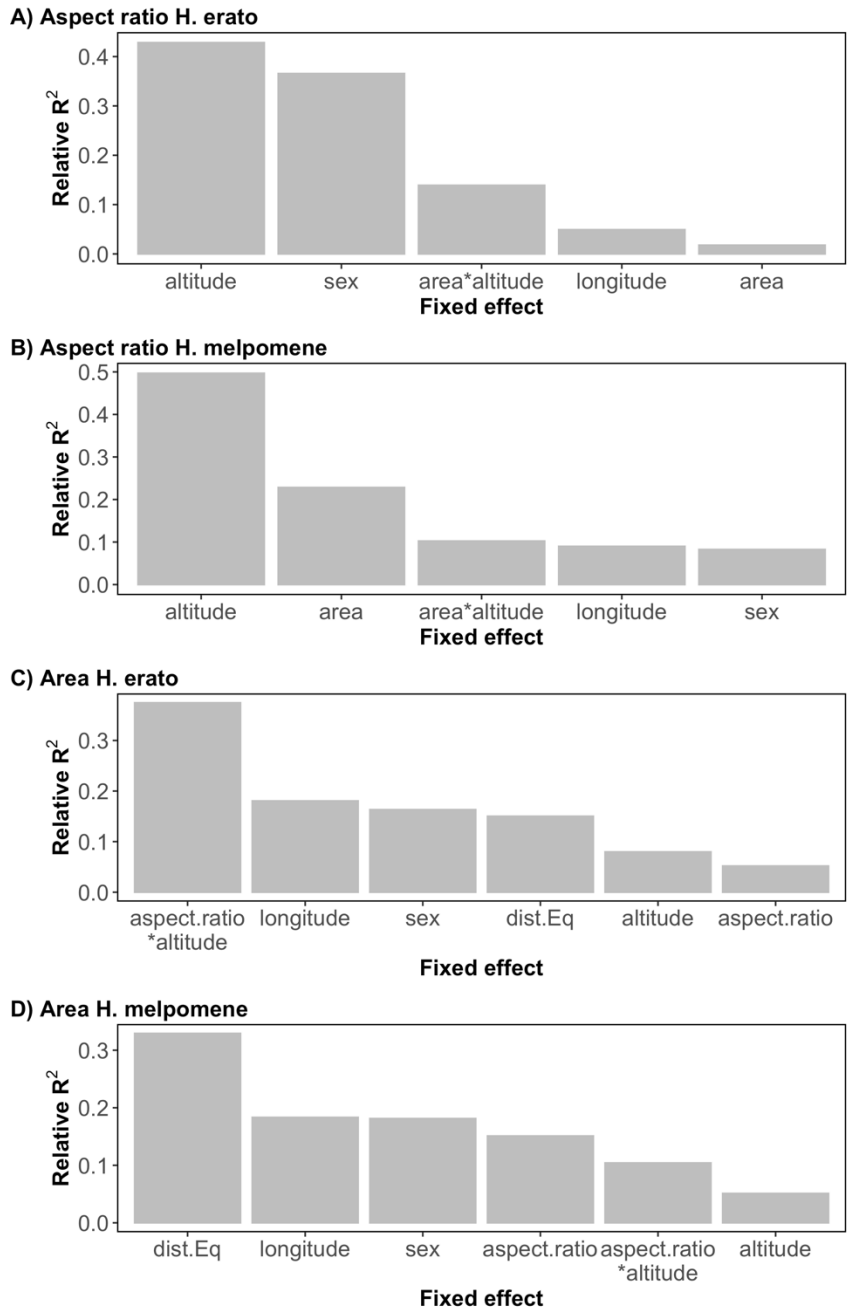
1040
 1041
 1042
 1043
 1044
 1045
 1046
 1047

Figure S11. Species variation in raw wing aspect ratio (A) and wing area (B) in *H. erato* (blue) and *H. melpomene* (orange). Points represent individual values. Lines show best linear fit for significant effects. Shaded areas show confidence bands at 1 standard error. Pearson correlation coefficients and p-values are shown for each regression plotted.



1048
 1049
 1050
 1051
 1052
 1053
 1054
 1055
 1056

Figure S12. Wing aspect ratio (A) and area (B) variation across mimicry ring wing patterns of the two most abundant species, *H. erato* (blue) and *H. melpomene* (orange). Error bars represent 95% confidence intervals of the means. Stars represent significance levels of two sample t-tests between *H. erato* and *H. melpomene* wings for each mimicry ring (•<0.08, *< 0.05, **<0.01, ***<0.001)



1057
 1058
 1059
 1060
 1061
 1062

Figure S13. Relative importance of model predictors of within species variation wing aspect ratio (A, B) and wing area (C, B) in *H. erato* (A, C) and *H. melpomene* (B, D). Total model adjusted R^2 values are A) 0.13, B) 0.14, C) 0.19, D) 0.19.

1063 **References**

1064

1065 Grömping, U. 2006. Relative Importance for Linear Regression in *R*: The Package

1066 **relaimpo**. Journal of Statistical Software, doi: 10.18637/jss.v017.i01.

1067 Keck, F., F. Rimet, A. Bouchez, and A. Franc. 2016. Phylosignal: An R package to

1068 measure, test, and explore the phylogenetic signal. Ecology and Evolution,

1069 doi: 10.1002/ece3.2051.

1070 Kozak, K. M., N. Wahlberg, A. F. E. Neild, K. K. Dasmahapatra, J. Mallet, and C. D.

1071 Jiggins. 2015. Multilocus species trees show the recent adaptive radiation of

1072 the mimetic heliconius butterflies. Systematic Biology 64:505–524.

1073

1074